IITRI

IIT Research Institute

IITRI Project No. G6021

CHARACTERIZATION OF CERAMIC MATERIALS

OR MICROELECTRONIC APPLICATIONS - PART III

tional Aeronautics and Space Administration
Langley Research Center, Mail Stop 126
Langley Station
Hampton, Virginia 23365

IITRI Project No. G6021

CHARACTERIZATION OF CERAMIC MATERIALS

FOR MICROELECTRONIC APPLICATIONS - PART III

National Aeronautics and Space Administration
Langley Research Center, Mail Stop 126
Langley Station
Hampton, Virginia 23365

NASA CR-66817

CHARACTERIZATION OF CERAMIC MATERIALS FOR MICROELECTRONIC APPLICATIONS - PART III

by

A. J. Mountvala

Prepared under Contract No. NAS1-8025
IIT RESEARCH INSTITUTE
10 West 35th Street
Chicago, Illinois 60616

for

NATIONAL AERONAUTICS AND SPACE ADMINISTRATION

IIT RESEARCH INSTITUTE

CHARACTERIZATION OF CERAMIC MATERIALS FOR MICROELECTRONIC APPLICATIONS - PART III

ABSTRACT

The major objectives of this investigation were to characterize surfaces and grain-boundaries in such electroceramic materials as $BaTiO_3$. Dielectric measurements over a frequency range were used to characterize particulate $BaTiO_3$ possessing known differences in stoichiometry and particle size. An electron beam scanning technique to study the electrical characteristics of ceramic grain-boundaries was developed, and results obtained with KCl and $BaTiO_3$ described.

CONTENTS

ILLUSTRATIONS

ILLUSTRATIONS (Cont'd)

ILLUSTRATIONS (Cont'd)

CHARACTERIZATION OF CERAMIC MATERIALS FOR MICROELECTRONIC APPLICATIONS - PART III

I. SUMMARY

Ceramics are used in microelectronic devices where they play an important role. Since their functions cannot be replaced, we have need to characterize them and, of course, predict their behavior, not only in use but in their fabrication. The question that comes up is, how. Unlike, say single crystal silicon, where an electronic engineer in semiconductor work can obtain well characterized data, and effectively design a usable device, no such information or even means of obtaining such data exists for ceramic materials.

Therefore, the major objectives of this investigation have been on the characterization of surfaces and grain-boundaries in electroceramic materials, such as barium titanate. This is so because the characteristics of surface layers of powders play a significant role in determining the processing and properties of materials, while the nature of grain-boundaries has a marked influence on the electrical behavior of sintered ceramics.

The work done on characterizing $BaTiO_3$ powders has shown how dielectric measurements can be used as a diagnostic tool for "finger-printing" the nature of particulate surfaces. Powder morphology and slight deviations in stoichiometry can be monitored by evaluating their ac conductivities as a function of partial pressure of water vapor. This is useful not only in the selection of starting powders for capacitor production but also for evaluating other ceramic powders such as mixed oxides, carbides, borides and nitrides, where stoichiometry can significantly alter electrical performance.

In fact, it is conceivable that this type of work could form the basis of a new chemical stoichiometry measuring instrument--a sort of "particle hydroxylmeter" analogous to potentiometer--

for determining stoichiometry of fine powders by evaluating the change in their conductivities as a function of water vapor. This would certainly be an attractive and a portable quality-control tool for raw material manufacturing.

The development and use of an electron beam scanning (EBS) system to study directly the electrical characteristics of grain-boundaries and interfaces have shown how boundary misorientations (twist and tilt), can alter the grain-boundary electrical conductivities in ionic materials such as KCl. In addition, the EBS data has shown that in $BaTiO_3$ ceramics the dielectric constant of "grain-boundary regions" is significantly different from that of the grains. This technique also has potential use as a manufacturing in-process control technique for evaluating junctions in active electronic devices.

Finally, the IITRI work on characterization of ceramic materials for microelectronic applications has evolved into new and somewhat different concepts on the methodology of characterization. The techniques developed on the NASA sponsored program are essentially "indirect" methods for characterization, which in many cases circumvent the complex and diverse variables that must be determined in "direct" characterization methods. Herein lies its practical usefulness as a manufacturing in-process control and design engineering technique.

II. INTRODUCTION

This is the final summary report on NASA Contract No. NAS1-8025 on "Characterization of Ceramic Materials for Microelectronic Applications". The report covers the period from March 13, 1968 to March 12, 1969.

The current program is aimed specifically at a meaningful characterization of electroceramic materials, such as $BaTiO_3$ which have significant applications in microelectronics. The research done at IITRI[1] under NASA Langley Research Center sponsorship has demonstrated that selected electrical measurements

can be applied to yield meaningful information about the interfacial (surfaces and grain-boundaries), and bulk properties of a ceramic such as $BaTiO_3$. The electrical measurements are not only pertinent to the end use of electroceramics in microelectronics, but simplify the interpretation of the electronic properties of the material for device design and microelectronic applications.

In attempting to characterize ceramic materials for microelectronic applications, we have directed our effort towards the following factors:

1. The properties of the surface layer of powder particulates and how they change with particle size, processing history and environmental partial pressure.

2. The electrical properties of the boundary phase in polycrystalline materials and their relationship to grain size and misorientation.

3. Possible correlation between the characteristics of the surface layer of the powder particles and those of the boundary phase in the ceramic.

III. CHARACTERIZATION OF $BaTiO_3$ POWDERS

A. Introduction

The characteristics of the surface defect layer of powders play a significant role in determining the properties of the sintered ceramic. Surface phenomena strongly affect particle size distribution and shape, its rheology in the forming operations, degasification during green body compaction, and finally, the sintering mechanism itself. All these factors are interrelated to the microstructure of the final ceramic, and hence affect its properties. With micron and submicron sized powders, because of the increased surface-to-volume ratio, the effects due to adsorbed gases and surface charges can alter the electronic behavior of the fired ceramic.

Generally speaking, the surface of a solid material is in an unusual crystallographic state due to valence requirements. In ceramic materials such as SiO_2 and Al_2O_3, the requirements of lowest free energy lead to a virgin surface ordinarily dominated by oxide ions which screen the less polarizable metal ions. Since inherently these surface ions have unsatisfied chemical valences, many of the bivalent surface oxide ions will attract positive-charged ions from the environment. Therefore the external surface of powders, and in particular of submicron sized material, can be considered as a defect structure. Such a defect layer involves a region adjacent to the outer surface boundary, physically and/or chemically adsorbed molecules and atoms on the surface, and electric fields extending away from the surface into the bulk.

Water vapor plays a significant role in determining surface phenomena of oxide powders. A number of investigators[2-4] have studied the surface hydration of various types of oxide powders using infrared adsorption and other techniques.

The possible role of the proton in the degradation process of titanates has been suggested by a number of investigators.[1,5] The proposed degradation mechanisms entailed proton generation at the anode and migration towards the cathode, or generation of anion vacancies. In either case, the electronic conductivity of the degrading titanate can be ascribed to the "hopping" of the 3d electrons of the Ti^{+3} ions. It is also possible that field-induced changes in electron distribution could be responsible for the degradation process.

However, not enough is understood about the effects of water vapor on micron and submicron sized $BaTiO_3$ powders. What are the nature of the defects as dehydration proceeds? Does the high energy surface strain condition on $BaTiO_3$ powders due to extensive dehydration, affect the polarization processes in the sintered material that is both ferroelectric and piezoelectric? From an electronic point of view, dehydration can be considered

analogous to charging a condenser, as the "dry surface" is assumed to have a different surface polarity than when covered with hydroxyl ions. What is the precise electronic structure of this outer defect layer? All these are unanswered questions that are pertinent to the characterization of $BaTiO_3$ powders.

It is the purpose of the study to explore some of the differences in the dielectric behavior due to water adsorption of $BaTiO_3$ powders with different particle size and surface characteristics.

To this end, scanning electron microscopy and dielectric measurements have been used as diagnostic tools to study the surface dominated behavior of barium titanate powders.

B. Experimental Procedures

Dielectric measurements were carried out on uncompressed and cold-compacted (unsintered) $BaTiO_3$ powders, under controlled water vapor environments.

The dielectric behavior of uncompressed powders was evaluated in a cell consisting of two concentric nickel cylinders embedded on end in a Teflon block--the powder under investigation being placed between the two concentric cylinders. Reproducibility of the cell was verified by measuring the capacitance and dissipation factor at 10^3 Hz of a powder specimen by filling and refilling the cell a number of times. Details and dimensions of this special cell have been described previously.[6] In order to emphasize the contribution of the surface layer, the dielectric properties reported in this study have been obtained on powders whose packing density in the dielectric cell gives a state of minimum compression, but commensurate with interparticle contact between the particulates.

The dielectric measurements on cold-compacted specimens (pressed at 10,000 psi external pressure), were carried out with a guarded ring electrode system.

The measurements were carried out in situ under controlled environments in a modified vacuum chamber. The partial pressure of water vapor, P_{H_2O}, was controlled by passing high-purity argon gas over drying columns of Drierite ($CaSO_4$), then Anhydrone ($Mg(ClO_4)_2$) to control P_{H_2O} at 7×10^{-6} atm, and over 85% and 45% strength H_2SO_4 solutions to obtain P_{H_2O} values of 7×10^{-5} atm, and 1.5×10^{-2} atm, respectively. The argon gas was bubbled through distilled water to obtain P_{H_2O} value of 3×10^{-2} atm.

To obtain equilibration, the specimens were exposed to each of the controlled atmospheres for about 70 hr prior to performing the electrical measurements.

In the isopropanol wash treatment the powders were thoroughly mixed with the alcohol, after which the solvent was removed at 400° under vacuum. The powder was then directly transformed to a glove-box with dry flowing He and measurements carried in situ.

All dielectric measurements were performed with a General Radio type 1615-A capacitance bridge. This bridge has at 10^3 Hz, a capacitance accuracy of $\pm 0.1\% + 0.00003$ pF, and a dissipation factor accuracy of $0.1\% + 10^{-5}$ of measured values. The frequency dispersion of the dielectric properties has been obtained over a range of 40 to 10^5 Hz.

In selecting $BaTiO_3$ powders for dielectric evaluation, emphasis was placed on the particle size and stoichiometry of the materials. However, it should be noted that these selected powders have different processing histories and not necessarily identical purity levels.

Material "C" is a 99.6% purity $BaTiO_3$ powder prepared by the Titanium Pigment Division, National Lead Company. Material "H" is a 99.1% purity experimental $BaTiO_3$ powder, which has a $BaO:TiO_2$ ratio corresponding to stoichiometry and is obtained from National Lead Company, TAM Division. Material "M" is a

high-purity $BaTiO_3$ powder obtained from the Air Force Materials Laboratory, Wright-Patterson Air Force Base. This material has been prepared by the controlled decomposition of metal alkoxides, and is reported[7] to have exact stoichiometry and an average particle size of about 0.01μ.

Scanning electron micrographs of $BaTiO_3$ powders were obtained with a Joelco model JSM scanning microscope. A thin gold film was deposited on all the particulate specimens to release electric charges prior to scanning.

The particle size distribution of powders "C" and "H" were determined by a Kaye Centrifugal Disc Photosedimentometer developed at IITRI. In this process, powder suspensions are passed through the photosedimentometer, in which the attenuation of light passing through the settling particles is measured and recorded on a strip chart. The chart data are programmed into a computer for final analysis. Figures 1 and 2 show the particle size distribution for the materials "C" and "H", respectively. The distribution at 0.5μ intervals is shown in Figures 3 and 4. Both powders show an average particle size of about 0.8μ, although "C" also has a slight bimodel distribution of larger size particles.

Surface area measurements were obtained by the BET technique. The $BaTiO_3$ samples were degassed to remove moisture and previously adsorbed gases at a temperature of 240° for 4 hrs. A steady stream of inert gas (He) was passed over the sample during degassing. Surface area was determined on a Perkin-Elmer Sorptometer which employs a continuous flow method. The results obtained on powders "C" and "H" are shown in Table I.

C. Scanning Electron Microscopy (SEM)

The SEM technique was used to study surface characteristics of $BaTiO_3$ powders and to obtain a possible correlation with their dielectric behavior.

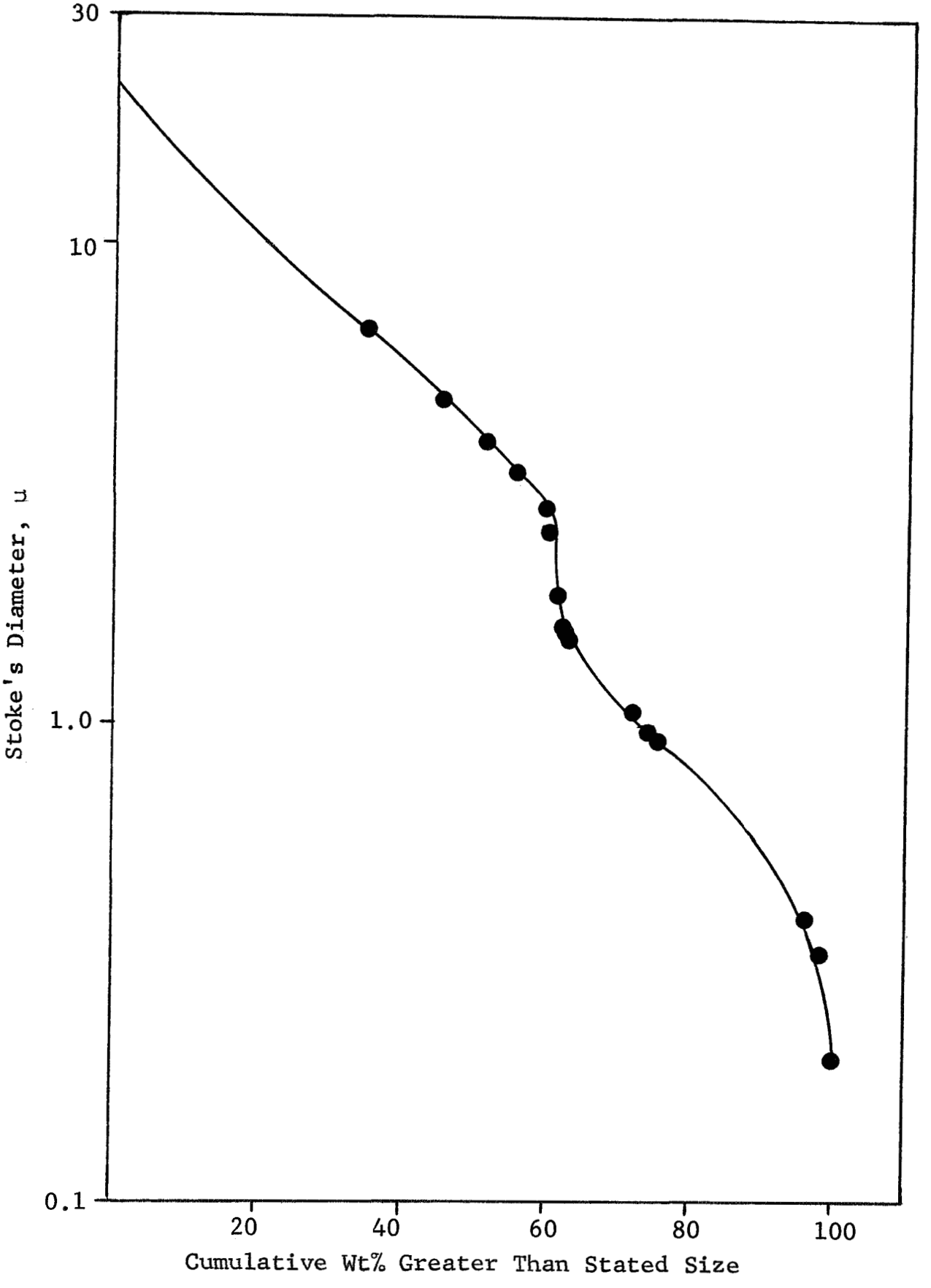

Fig. 1 PARTICLE SIZE DISTRIBUTION OF $BaTiO_3$ POWDER - MATERIAL C

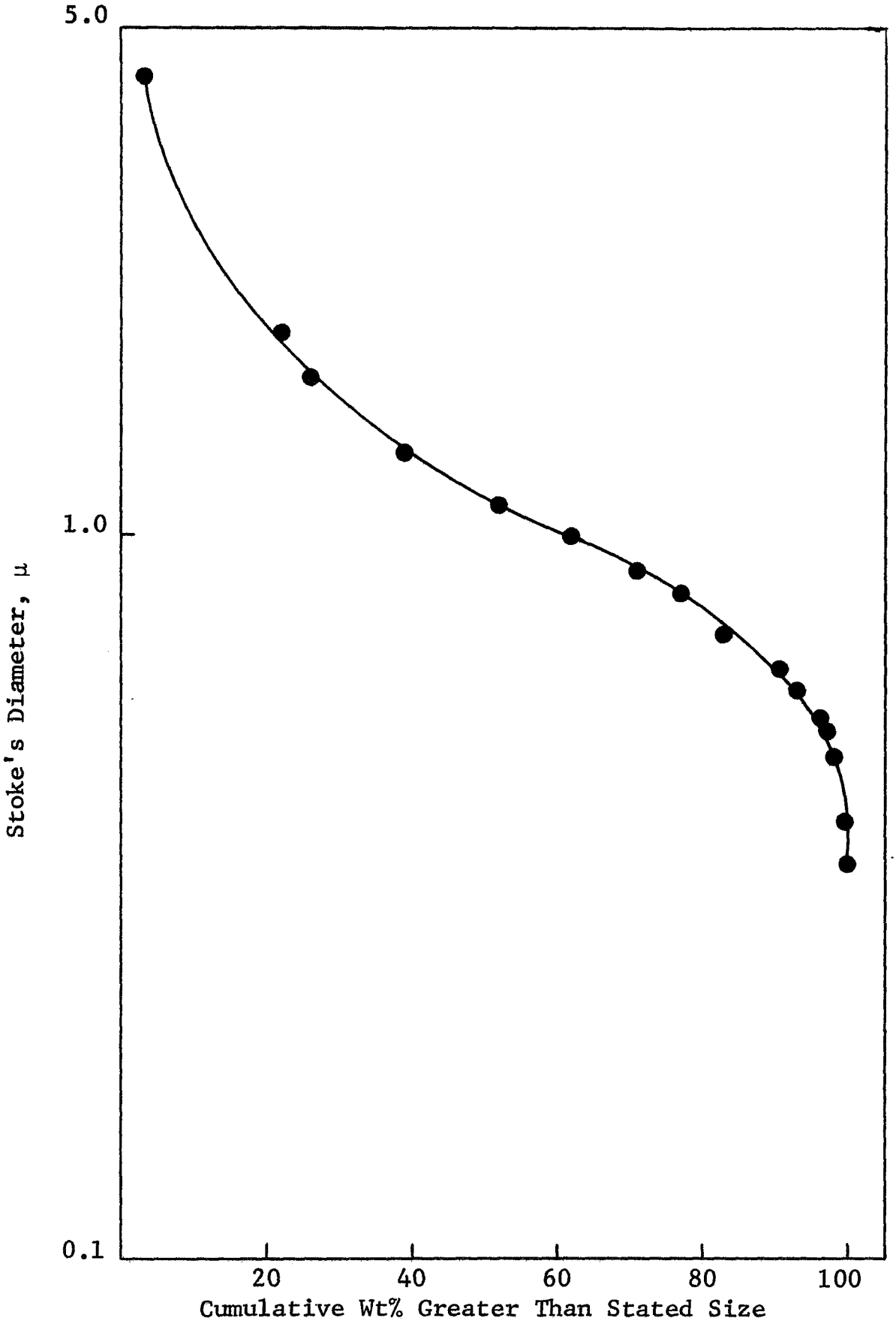

Fig. 2 PARTICLE SIZE DISTRIBUTION OF $BaTiO_3$ POWDER - MATERIAL H

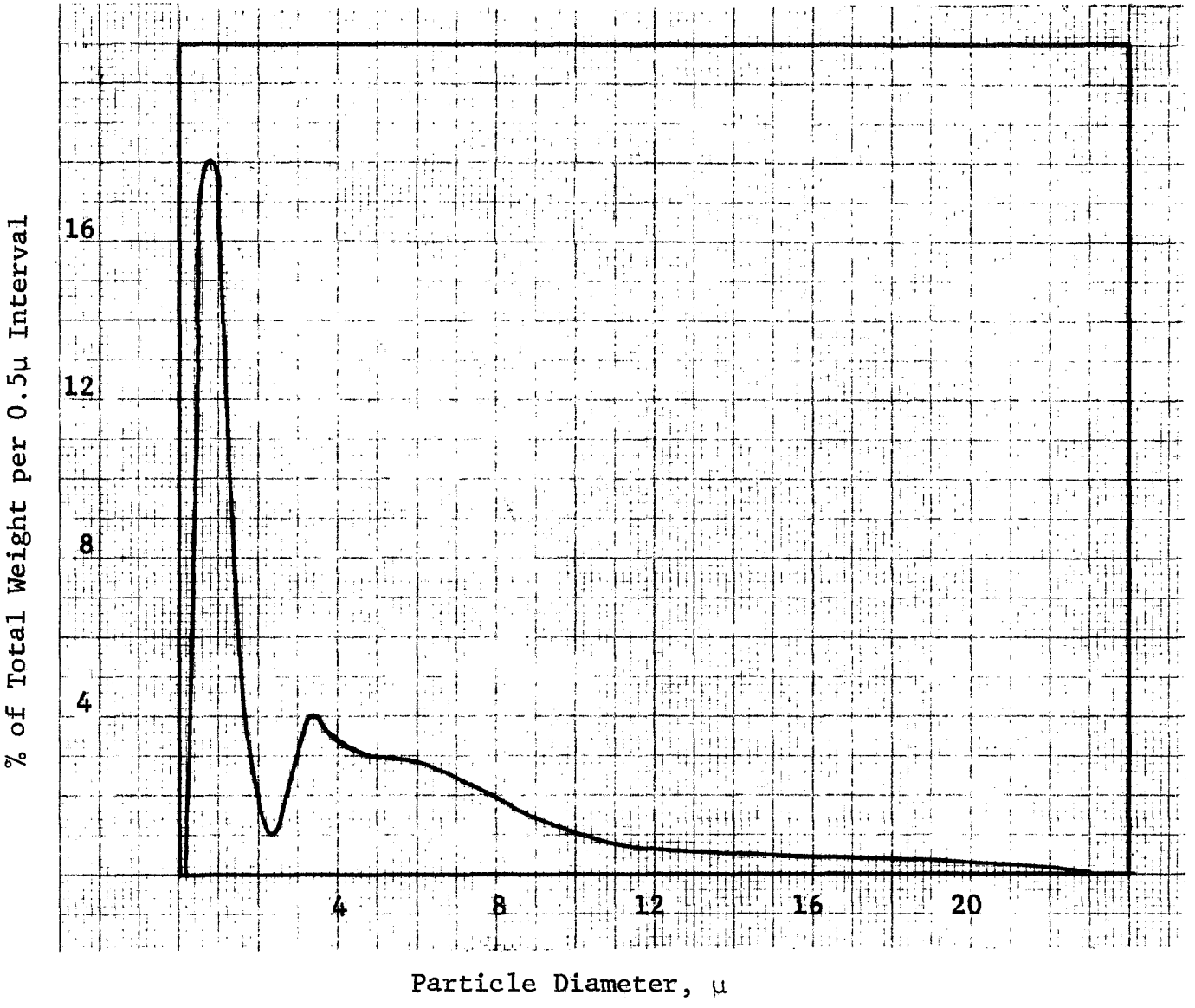

Fig. 3 PARTICLE SIZE DISTRIBUTION FOR $BaTiO_3$ MATERIAL C, FOR 0.5μ INTERVALS

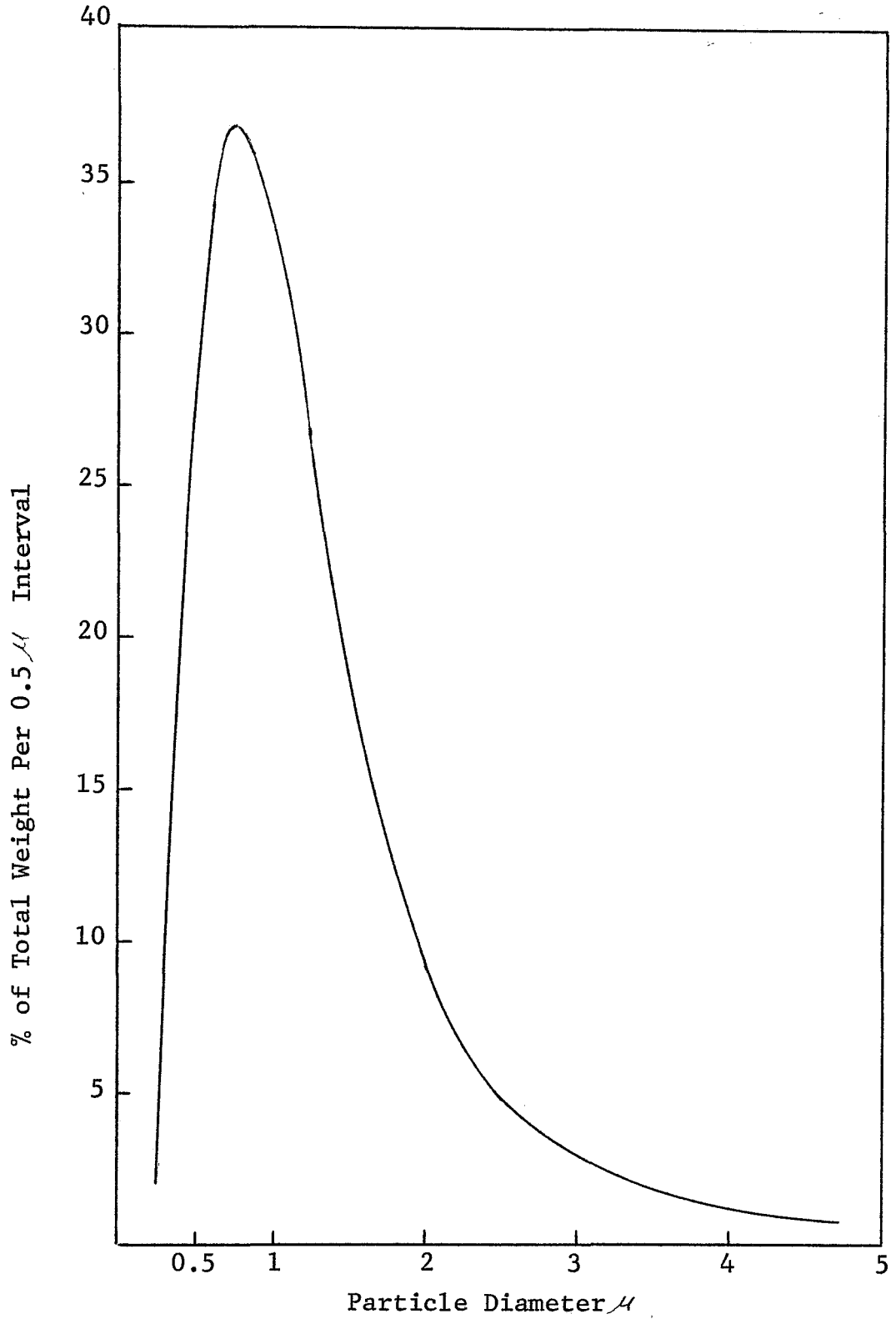

Fig. 4 PARTICLE SIZE DISTRIBUTION FOR $BaTiO_3$ MATERIAL H FOR 0.5μ INTERVALS

Table I

CHARACTERISTICS OF $BaTiO_3$ POWDERS

	$BaTiO_3$ "C"	"H"	"M"
Average particle size (μ)	0.8	0.75	0.01
Surface area (m^2/g)	4.91	3.2	———
$BaO:TiO_2$ ratio	0.995	1.001	1.000

Figures 5 to 9 are scanning electron micrographs of powder "C". Figure 5 shows the presence of two types of particle clusters indicated by "A" and "B". Figures 6 and 7 show cluster "A" at 10,000X and 20,000X magnifications, and is indicative of a highly "defective" surface topography. It is not clear at this time as to what extent the particles are agglomerated in these clusters. Figure 8 shows the particles obtained by scanning another portion of the original powder specimen. They are similar to the particles observed in cluster "A" (Figure 5). Figure 9 shows cluster "B" at 6,000X magnification. Some of the particles seem to be rod-like and different from the majority of particles observed in this powder. This is in agreement with data on particle size distribution where a bimodel distribution was obtained.

In contrast, Figure 10 shows the scanning electron photomicrograph of $BaTiO_3$ material "H". This powder appears to have a surface topography significantly different from the "defective" type characteristic of material "C".

Material "C" is $BaTiO_3$ prepared by thermal decomposition of barium titanyl oxalate. Typically, this material consists of relatively large particulates which are composed of much smaller crystallites. This of course gives rise to a somewhat porous structure, as confirmed by the SEM results.

The second type of material ($BaTiO_3$ "H") was prepared from the decomposition of barium carbonate with titania, and SEM results show that it has a well defined cube-like crystallite structure.

Dielectric measurements discussed in the following section indicate a possible correlation between the surface character and effects of water vapor on dielectric behavior.

The fine particle size ($\sim$0.01) of material "M" is shown in Figure 11.

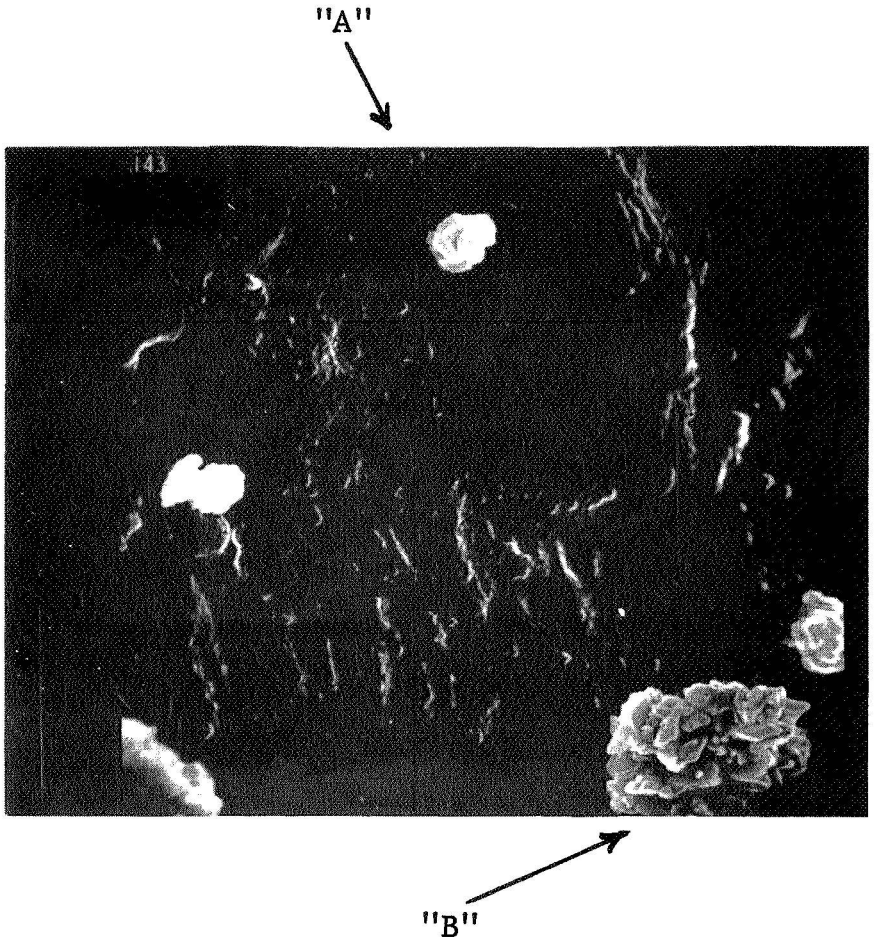

Fig. 5 SCANNING ELECTRON MICROGRAPH OF $BaTiO_3$ POWDER "C" (2000X)

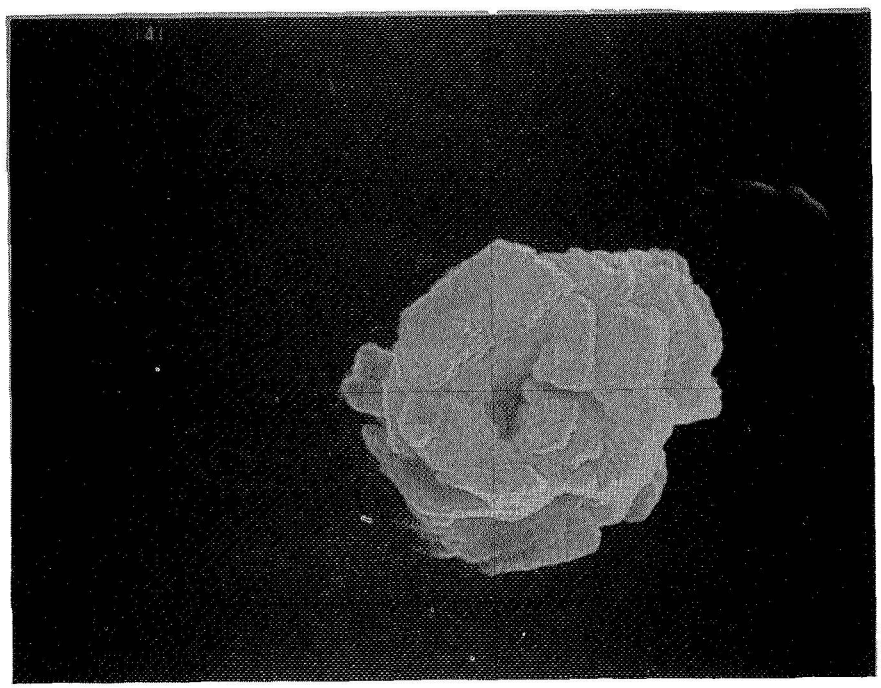

Fig. 6 - SCANNING ELECTRON MICROGRAPH OF $BaTiO_3$ POWDER "C" SHOWING CLUSTER "A" (10,000X)

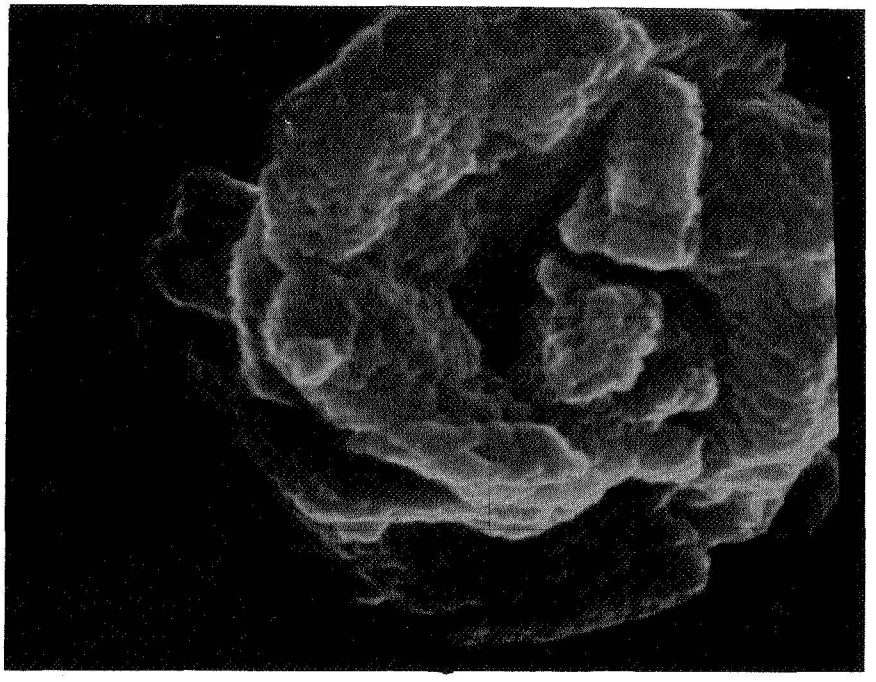

Fig. 7 - SCANNING ELECTRON MICROGRAPH OF $BaTiO_3$ POWDER "C" SHOWING CLUSTER "A" (20,000X)

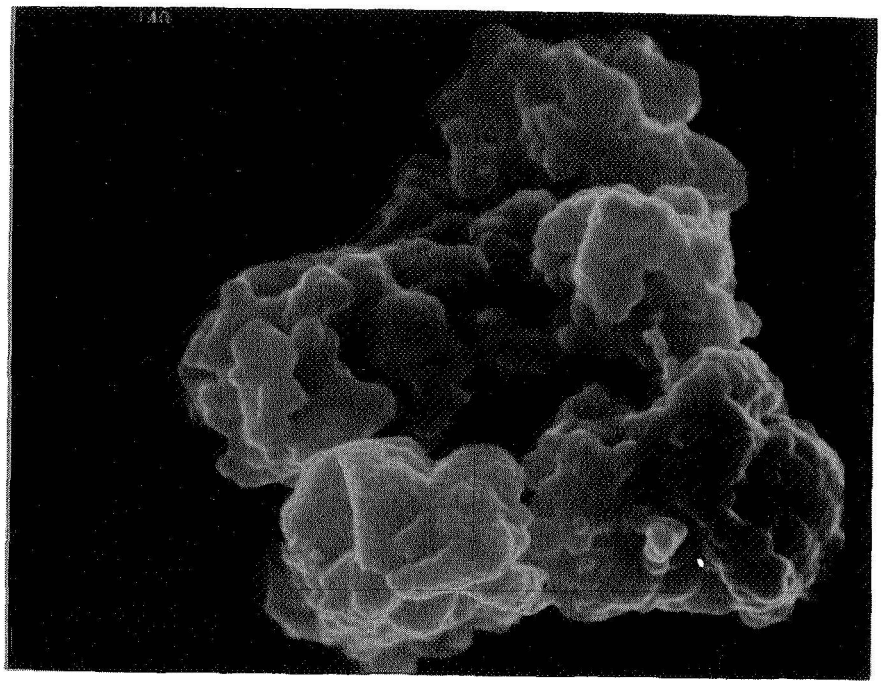

Fig. 8 - SCANNING ELECTRON MICROGRAPH OF $BaTiO_3$ POWDER "C" (10,000X)

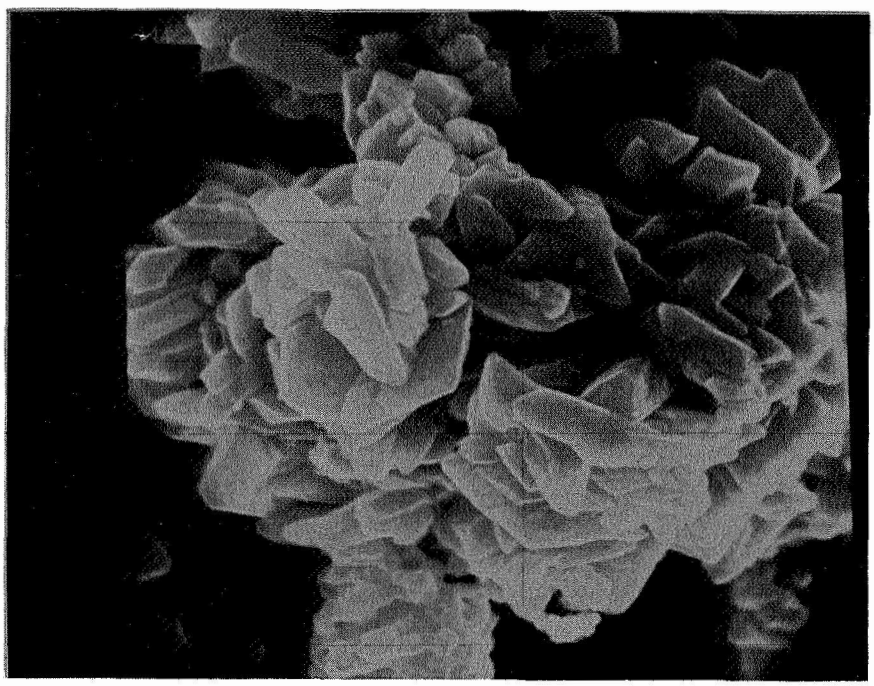

Fig. 9 - SCANNING ELECTRON MICROGRAPH OF $BaTiO_3$ POWDER "C" SHOWING CLUSTER "B" (6,000X)

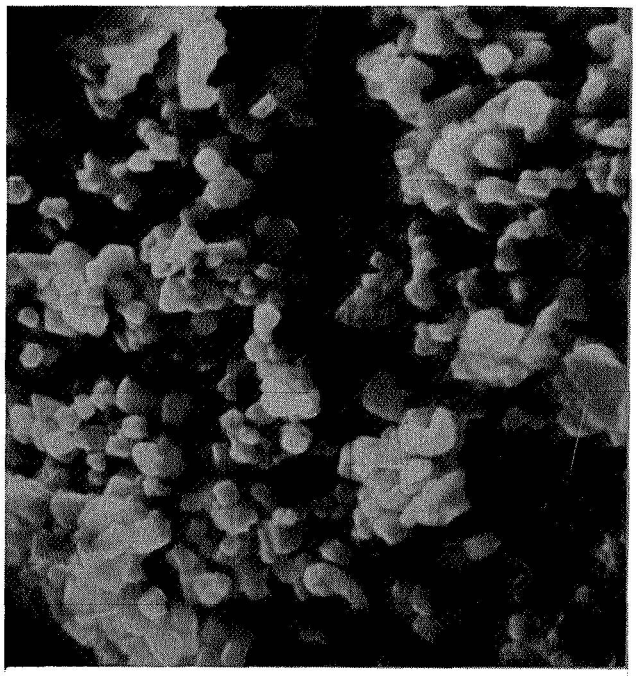

Fig. 10 - SCANNING ELECTRON MICROGRAPH OF $BaTiO_3$ POWDER "H" (X10000)

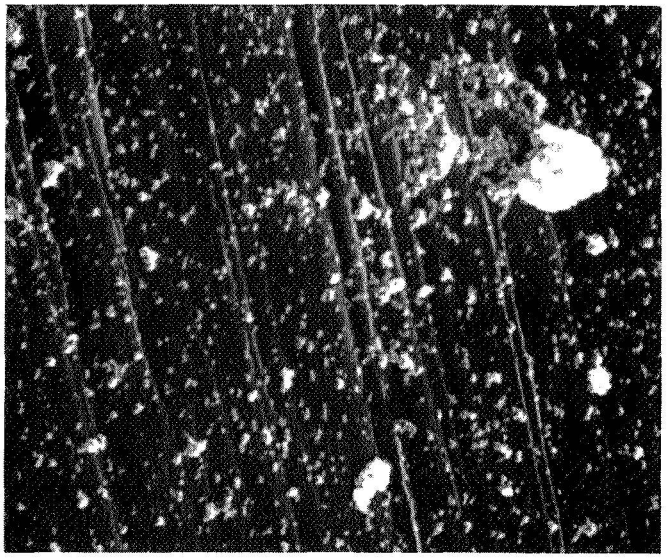

(X5000)

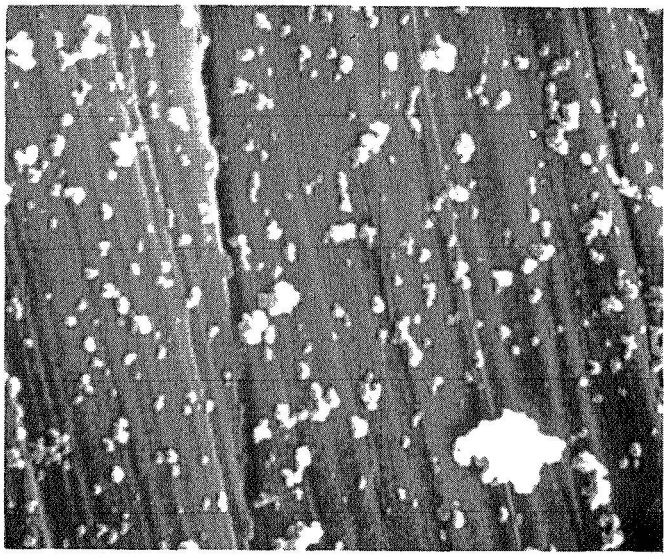

(X10,000)

Fig. 11 SCANNING ELECTRON MICROGRAPH OF ULTRA FINE PARTICLE SIZE (0.01) $BaTiO_3$ POWDER "M"

Scanning electron microscopy was also used to determine the manner in which an organic binder (1.5% cellulose acetate plus 6% dibutyl phthalate), interacts with $BaTiO_3$ powder material "H". Figure 12 illustrates the marked difference in structure observable before and after the introduction of a binder and provides an insight into what happens during processing of $BaTiO_3$. It should be noted that the chemistry and physics of ceramic-binder interaction is not well understood, and the role of binder is understood only on an empirical basis.

D. Dielectric Behavior

The significance of surface activity for ultrafine sized ($\sim 0.01\mu$) $BaTiO_3$ powders (material "M"), is illustrated by the frequency dispersion of the dielectric properties shown in Figures 13, 14, and 15. These results can be rationalized with a model where the surface properties predominate, especially at lower frequencies. The fine particle powder due to its large surface area-to-volume ratio would tend to adsorb gaseous species, in particular hydroxyl groups, in the as-received state. The subsequent change in the frequency dispersions of relative permittivity (ϵ_r), imaginary part of permittivity (ϵ''), and dissipation factor ($\tan\delta$) by subjecting the $BaTiO_3$ powder to an isopropanol wash can be ascribed to the removal of surface bound hydroxyl groups. Thus, the isopropanol treatment is purported to give a product with a "clean" surface and a material with reduced dielectric loss characteristics. With the recent advent of using ultrafine size electroceramic materials for high K'-capacitors and substrates, this effect is of significance to raw material vendors and capacitor manufacturers.

We have hypothesized that the chemically adsorbed isopropanol groups combine with a proton to depart as molecules of isopropanol in a process analogous to surface dehydration, as shown below:

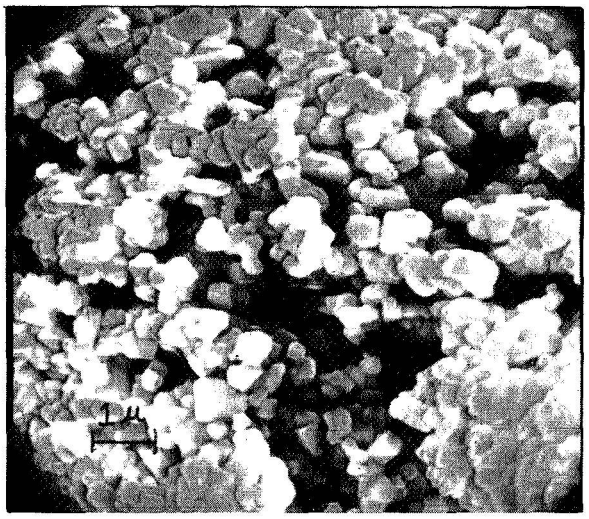

b

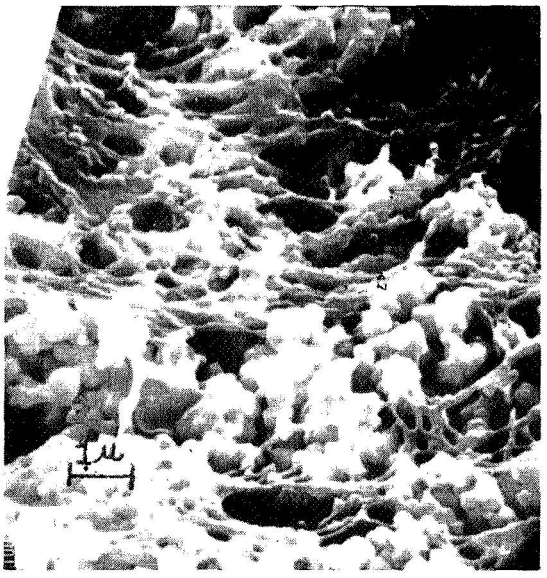

a

Fig. 12 SCANNING ELECTRON MICROGRAPHS OF $BaTiO_3$ PARTICULATES
(a) Showing Distribution of Organic Binder and
(b) Without (10,000X)

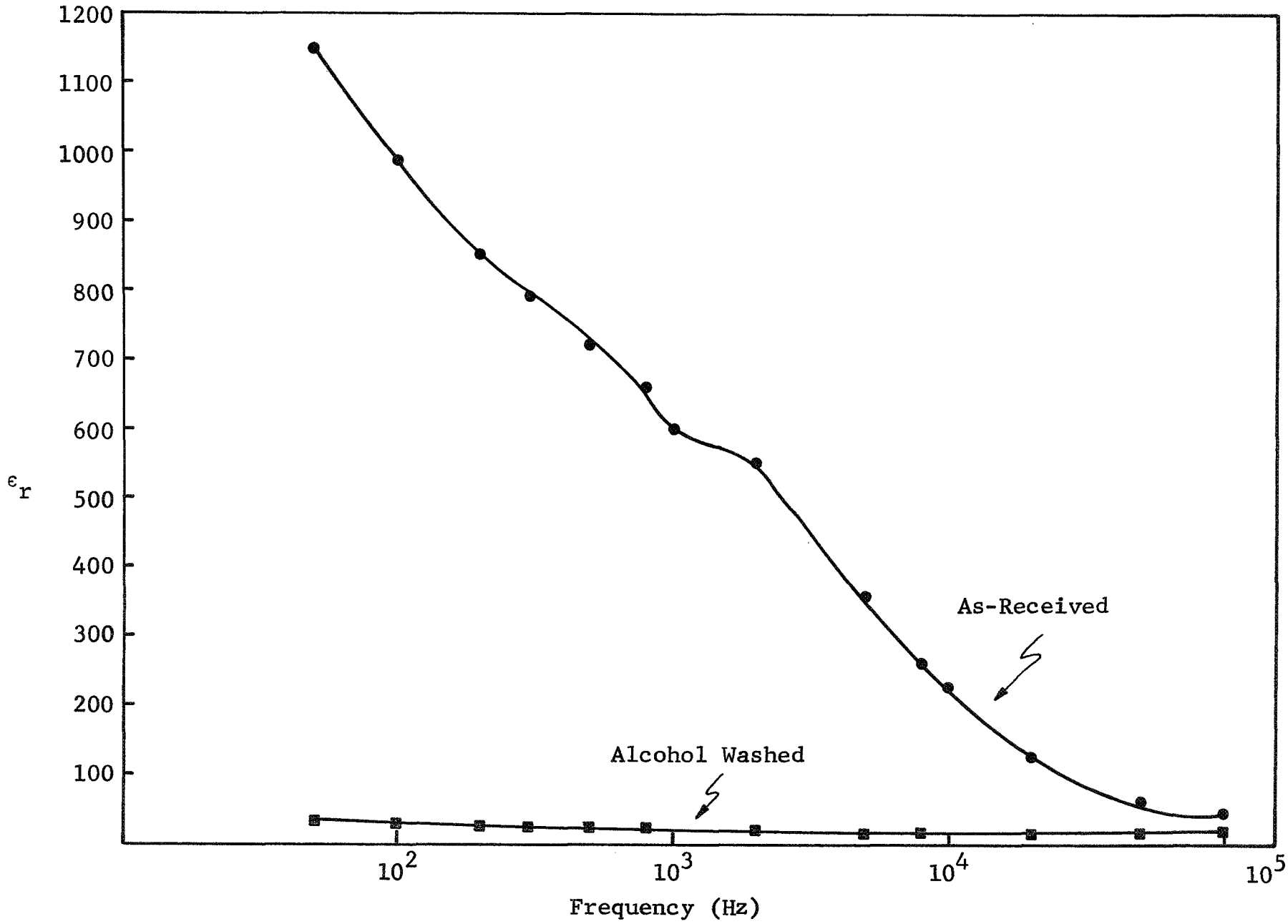

Fig. 13 FREQUENCY DEPENDENCE OF RELATIVE PERMITTIVITY (ϵ_r) OF ULTRAFINE SIZE $BaTiO_3$ POWDER "M" (Meas. in dry helium)

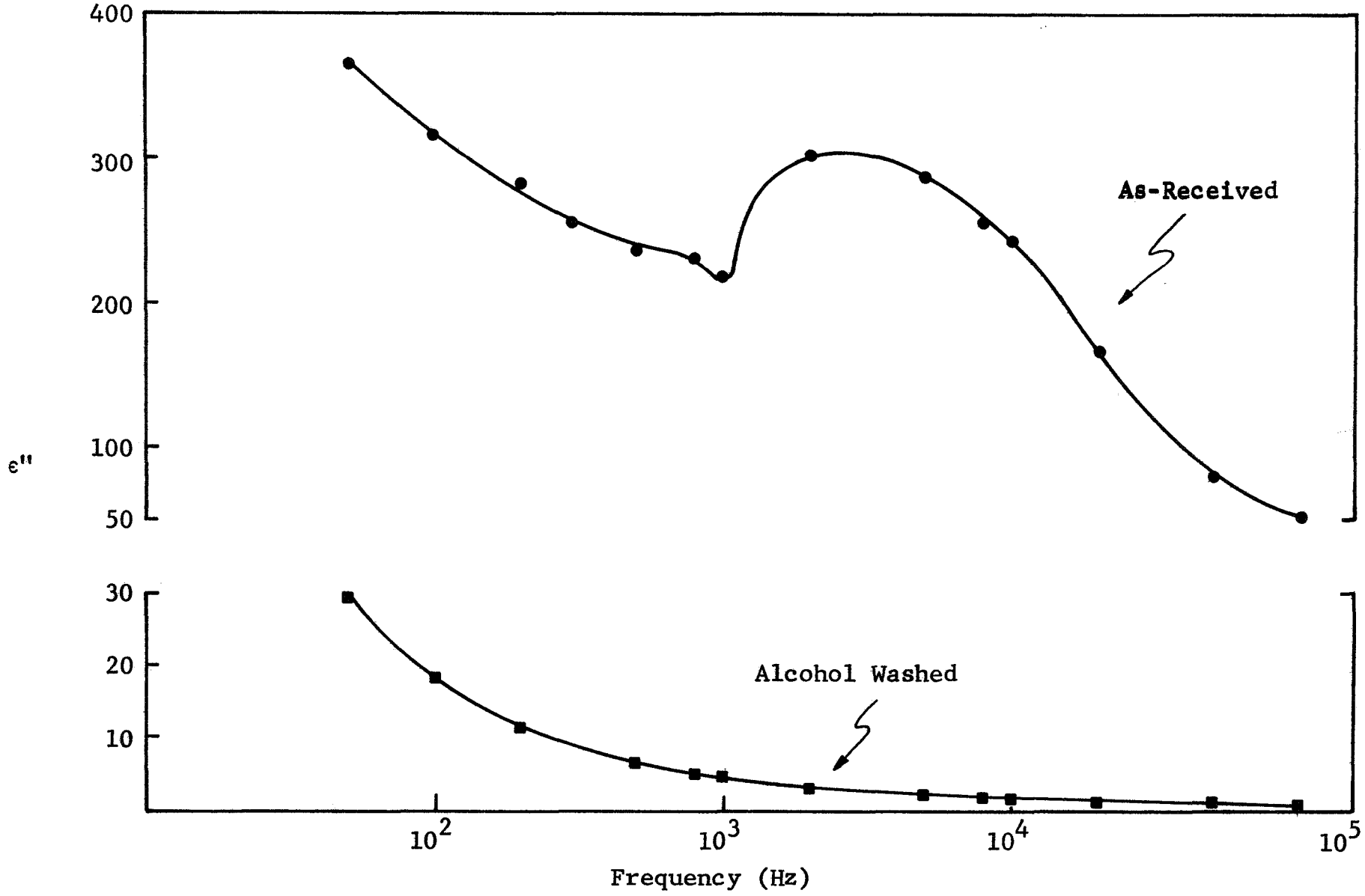

Fig. 14 FREQUENCY DEPENDENCE OF IMAGINARY PART OF PERMITTIVITY (ε'') OF ULTRAFINE SIZE $BaTiO_3$ POWDER "M" (Meas. in dry helium)

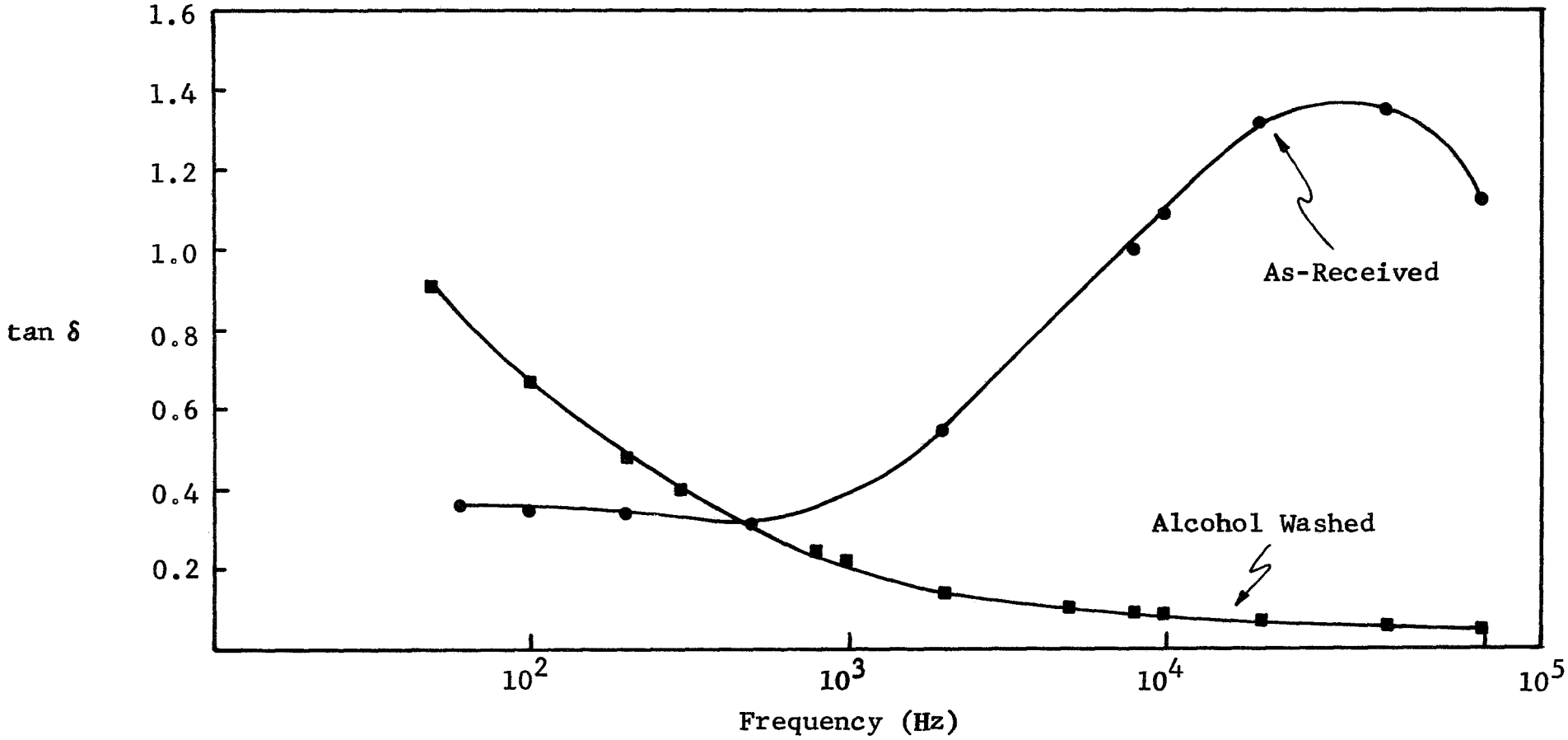

Fig. 15 FREQUENCY DEPENDENCE OF DISSIPATION FACTOR (tan δ) OF ULTRAFINE SIZE $BaTiO_3$ POWDER "M" (Meas. in dry helium)

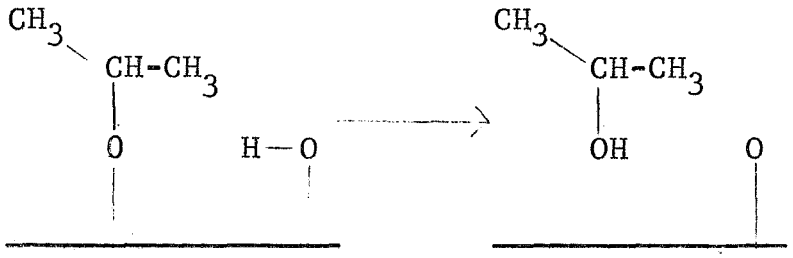

The absence of a low frequency dispersion of ϵ_r, ϵ'' and $\tan\delta$, after the alcohol treatment (wash followed by removal at 400°C), tends to indicate that the isopropanol effectively dehydrates the barium titanate surface. A similar effect has been observed for alumina powders.[6]

In view of these results, it is meaningful to ask whether the dielectric properties of $BaTiO_3$ powders are particle size dependent for "clean" surfaces.

Figure 16 shows the relative permittivity (ϵ_r) corrected for porosity of two types of $BaTiO_3$ powders, "H" and "M", with average particle sizes of 1.0 and 0.01μ, respectively, after being subjected to the isopropanol treatment. These two materials are supposed to have a $BaO:TiO_2$ ratio equal to one according to suppliers. The measurements were performed in situ in a dry He atmosphere, such that the powders were not exposed to air after the alcohol wash. The data indicates that although the 0.01μ particle size $BaTiO_3$ (AFML material) has a slightly higher permittivity value than the 1.0μ particle size material ("H"), there are no significant differences in their relative permittivities in comparison with the marked difference in their particle sizes. It should be remembered that the 0.01μ particle size $BaTiO_3$ has much higher ϵ_r values in the "as-received" state or when exposed to air.

The measured values of loss tangent ($\tan\delta$) for the two types of powders were not found to be significantly different either, after the "alcohol wash" treatment.

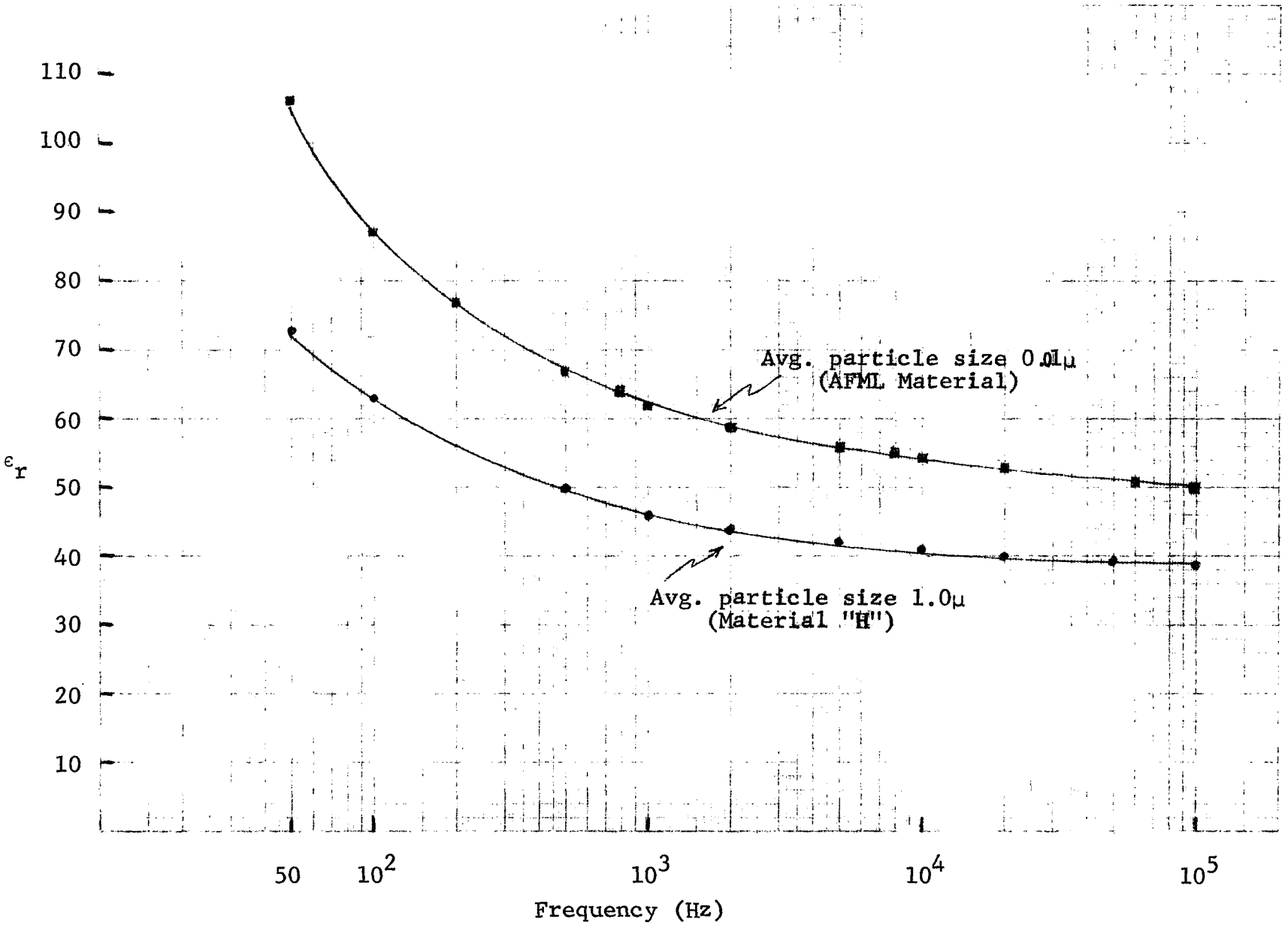

Fig. 16 FREQUENCY DEPENDENCE OF RELATIVE PERMITTIVITY (ϵ_r) OF $BaTiO_3$ POWDERS AFTER "ALCOHOL WASH" TREATMENT (Meas. in Dry Helium)

The results described above if interpreted by themselves tend to indicate that the previously reported[8] particle size dependence of dielectric constant for $BaTiO_3$ powders is not an intrinsic surface layer characteristic, but primarily due to the difference in surface reactivity or degree of hydroxylation caused by varying surface area-to-volume ratios. Further, it seems that a particle size dependence does not exist for "clean" surfaces. However, it should be remembered that these powders were prepared by significantly different techniques and have different impurity levels.

The effect of water adsorption at 25°C on the dielectric behavior of two contrasting samples of $BaTiO_3$ powders, namely "C" and "H", have been investigated. Although the average particle size of the two samples were approximately equal (0.8 to 1.0μ), their surface "character" (surface topography and areas), and stoichiometry were markedly different. The reported data has been obtained on cold-compacted (unsintered) specimens with identical packing densities (54% of the theoretical).

The frequency dispersion of the dielectric constant K' of the cold-compacted specimens at various P_{H_2O} values has been shown in Figures 17 and 18. Water vapor at partial pressures of about 1.5×10^{-3} atm and above causes a significant increase in the dielectric constant, especially at lower frequencies ($\lesssim$ 1 kHz).

The effects of the water partial pressure on the ac conductivity (σ_{ac}) of the powders is shown in Figure 19. The results show that material "H" shows a significant change in σ_{ac} at values of $P_{H_2O} \geq 10^{-3}$ atm. The data obtained on material "C" (specimen no. C-1p) indicates that in spite of the lack of equilibration discussed below, the σ_{ac} is more sensitive to changes in P_{H_2O} values than for similar specimens prepared from material "H". The conductivity values have been obtained by exposing the test specimen for 72 hrs at each successive partial pressure of water. This time period was sufficient for equilibration at the

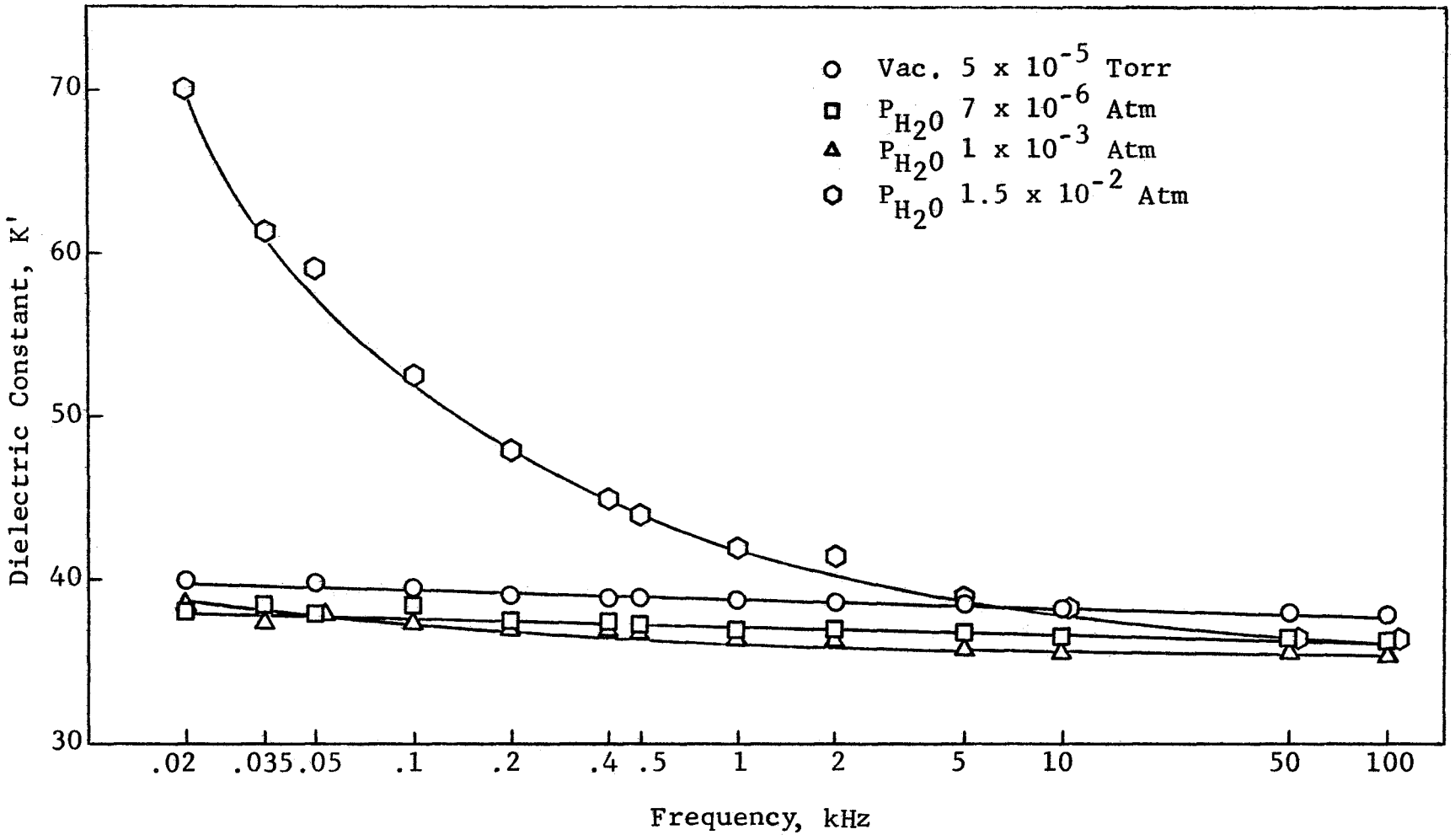

Fig. 17 EFFECT OF P_{H_2O} ON DIELECTRIC CONSTANT K' OF SPECIMEN H-1p

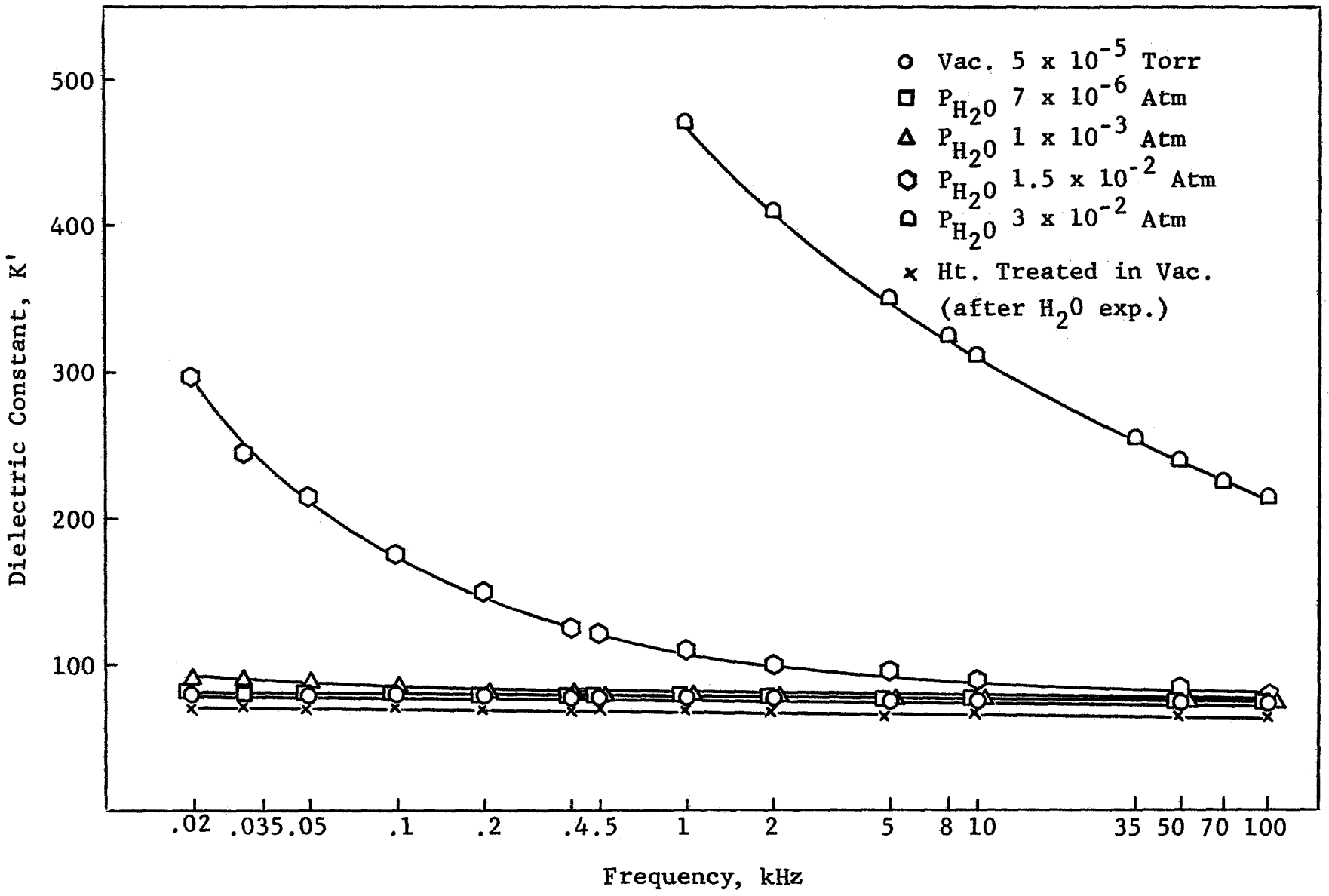

Fig. 18 EFFECT OF P_{H_2O} ON DIELECTRIC CONSTANT K' OF SPECIMEN C-1p

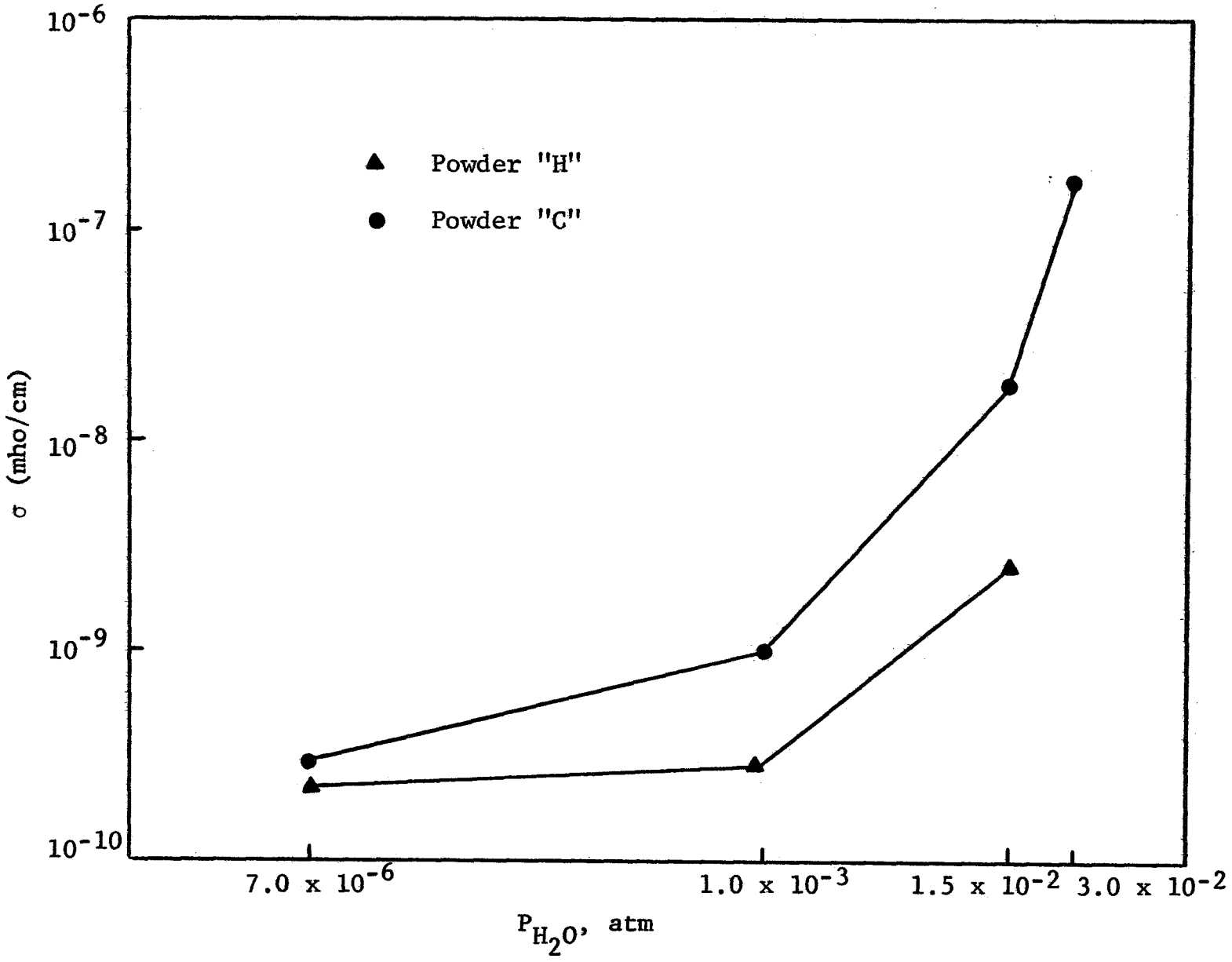

Fig. 19 EFFECT OF WATER VAPOR ON AC CONDUCTIVITY OF $BaTiO_3$ POWDERS (MEASURED AT 1kHz)

lower P_{H_2O} value of 1 x 1.0^{-3} atm, and no changes in occurred for exposure times ranging from 48 to 120 hrs. For higher P_{H_2O} values a slight change in was obtained for the porous cold-compacted specimen (H), while the porous cold-compacted (C) prepared from material "C" did show a change in values for exposure times of 48 to 72 hrs, indicating that equilibration had not taken place.

It should be noted that the barium titanate powders having differences in their surface structure show significantly different dielectric loss phenomena due to water vapor, but have nearly identical values of D and $_{ac}$ at a P_{H_2O} value of 7 x 10^{-6} atm and in vacuum (10^{-6} torr). The enhanced dielectric loss in the material with a slight excess of TiO_2 (C) as compared to the stoichiometric material (H), only manifests itself with increasing partial pressure of H_2O as shown in Figure 19.

A number of possible reasons exist for the differences in dielectric loss behavior due to water vapor for materials "C" and "H".

The adsorption of gases on particulate ceramics is affected by the size, shape, surface area, and charge distribution at the surface of the particles. Both powders were found to have very similar average particle size (0.8), and the test specimens had identical densities (54% theoretical) and dimensions.

However, powders "C" and "H" do have different surface areas of $4.9m^2/g$ and $3.2m^2/g$, respectively. In addition, SEM studies indicated that they possess markedly different surface topography. The powder showing the enhanced dielectric loss due to water adsorption also has a highly defective surface topography.

The fact that the dielectric loss evaluations were carried out on cold-compacted specimens of about 54% of theoretical bulk density and not on dispersed powders could somewhat reduce

the significance of possible differences in surface area per unit volume, especially for powders having very similar particle sizes.

Impurity effects could change the dielectric loss characteristics of $BaTiO_3$. Both materials "C" and "H" are developmental type powders and have significantly higher purities than commercial $BaTiO_3$. However, differences in impurity content of multivalent ions such as iron could change the loss characteristics. A partially complete spectroscopic analysis indicates that the Fe_2O_3 content is < 0.001 and 0.012 wt% respectively for materials "C" and "H", and that in general material "C" which shows the enhanced dielectric loss due to water vapor, is a purer material than "H" which had reduced loss characteristics. Therefore, impurity effects cannot explain the observed differences in dielectric loss due to interaction in the water vapor.

It has been recognized that the effects of stoichiometry in $BaTiO_2$ are significant, and in some cases more important than the attainment of higher purity. Barium titanate material "C" has a BaO/TiO_2 ratio of 1.001, while material "H" has a $BaO:TiO_2$ ratio of 0.995. Therefore, the possibility that a greater number of surface defects are created due to interaction with water vapor in material "C", which has a slight excess of TiO_2 as compared to material "H" which does not have excess TiO_2, must be considered. If this is so, it offers an exciting potential of monitoring very small deviations in stoichiometry, particularly in ultra fine particle size materials from significant changes in the ac conductivity as a junction of partial pressure of water.

However, these results do indicate that the surfaces of barium titanate powders can be characterized by evaluating the changes in ac conductivity due to controlled partial pressure of water.

IV. USE OF ELECTRON BEAM SCANNING (EBS) TECHNIQUE FOR DIRECT MEASUREMENT OF DIELECTRIC PROPERTIES OF GRAINS AND GRAIN-BOUNDARIES

A. Introduction

The electron beam scanning (EBS) technique is a new and direct approach to the study of the dielectric properties of grain-boundaries and interfaces.

The EBS system, developed at IITRI, was first constructed in 1965 and has been described previously.[9] In this technique, one surface of the dielectric material is charged with a scanning electron beam in a vacuum. The charge measurement is obtained in the form of a video signal output, which is a measure of the spatially resolved conductivity of the sample. The use of an electron beam to produce an equipotential insulator surface has several desirable features. The charging source is basically high impedance. Beam currents are easily measured and controlled, and excellent guarding of the measurement area occurs automatically for most scanning patterns. For a study of grain-boundaries and interfaces, its most significant feature is that the area of dielectric evaluation is of the order of the electron beam spot size and can be made very small. This, coupled with the ability to move the area of measurement to various positions on the sample in a simple manner, makes it a unique tool for studying the dielectric properties of grain-boundaries as a function of grain size, stoichiometry and other microstructural parameters.

An attempt has been made to adapt the existing EBS system for studying the dielectric properties of grain-boundaries in potassium chloride and barium titanate. Preliminary experiments were performed on potassium chloride (KCl) bicrystals and barium titanate ($BaTiO_3$) multicrystalline specimens. The bicrystal specimens were used for these experiments as they offer a single grain-boundary with well defined boundary misorientations, which is advantageous in developing and modifying the EBS circuitry

to meet this program's objectives. In addition, the alkali halides can be considered as model materials for certain oxides such as MgO.

B. Experimental Procedure

The mechanical arrangements for dielectric measurements using this technique are straight forward. Figure 20 is a schematic diagram of the EBS system. The sample is backed on one side by a metallic electrode while the other side is irradiated by an electron beam produced by a conventional electron gun. A collector grid or a large diameter collector ring is placed close to the sample. The collector electrode may be at ground potential, and the backing electrode is connected to a variable high-voltage supply initially at ground potential. If the electron accelerating potential is of the order of several hundred volts, and if the secondary electron emission coefficient (δ_{eff}) of the insulator is greater than unity at this voltage then initially, the potential of each spot on the insulator which is bombarded by the primary beam will tend to change from zero to a positive value. The sample surface potential will come to an equilibrium value of a few volts above ground, when $\delta_{eff} = 1$. The sample is then no longer being charged. If the backing electrode is then slowly raised to a high potential of either polarity while the electron beam continues to scan the sample in a regular pattern, each spot on the front surface of the sample will be brought back to the same equilibrium potential whenever the beam strikes it. The charge deposited on the sample will be opposite in polarity to that of the high-voltage backing electrode and of a magnitude sufficient to charge the sample capacitance to the potential difference between its surfaces, and also to compensate for the conduction which has occurred between its surfaces.

The determination of dielectric properties depends on knowing the voltage drop across the sample and the charge deposited on the sample by the electron beam.

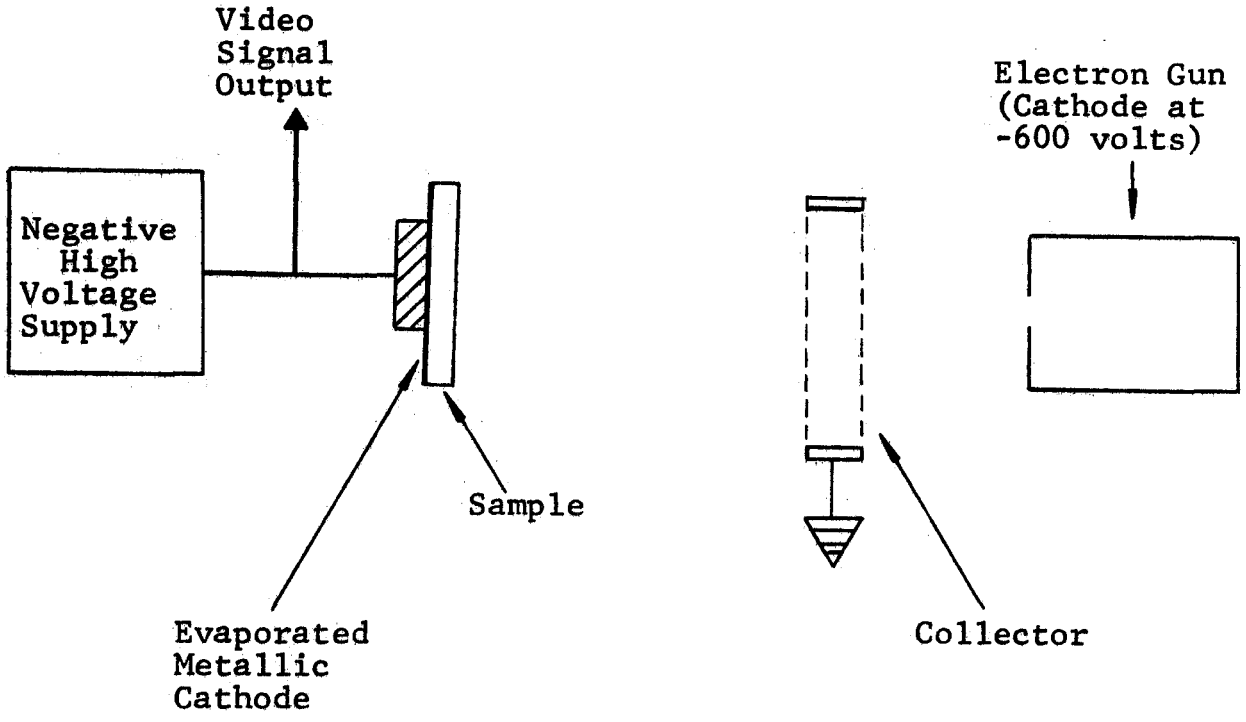

Fig. 20 SCHEMATIC DIAGRAM OF THE ELECTRON BEAM SCANNING SYSTEM

The $BaTiO_3$ used in these experiments was a 50 mil thick multicrystalline specimen obtained from an imperfect portion of a high purity $BaTiO_3$ single crystal boule. This multicrystalline specimen was selected because it has large crystals with well defined boundaries. The specimen holder shown in Figure 21, was designed to optimize readout and minimize secondary electron effects.

The KCl bicrystals were about 10 mil thick with well defined boundary misorientations and were tested in a holder as shown in Figure 22. Figure 23 shows four KCl crystals of different boundary misorientations mounted together in a holder.

C. Results and Discussion

1. Grain Boundary Profiles

The major experimental objectives were: firstly, to determine whether it is possible to separate sufficiently the dielectric properties of conductivity and dielectric constant from secondary electron emission effects, so as to be able to observe the relative variations of these dielectric properties as a function of specimen position in the EBS technique. And subsequently, to ascertain whether the dielectric properties of the grain-boundary region are sufficiently different from those of the grain, so as to observe a conductivity and/or dielectric constant profile of the grain-boundary region.

Experimental effort was first directed toward the separation of the extrinsic secondary emission effects from the dielectric properties on the KCl bicrystal specimen. It is to be realized that differences in the secondary emission coefficient and secondary redistribution lead to charging of the specimen in ways which may or may not have any relation to its dielectric properties. If changes in charging and patterns of charge distribution resulting from these secondary electron emission effects are larger than those produced by the intrinsic dielectric properties of the

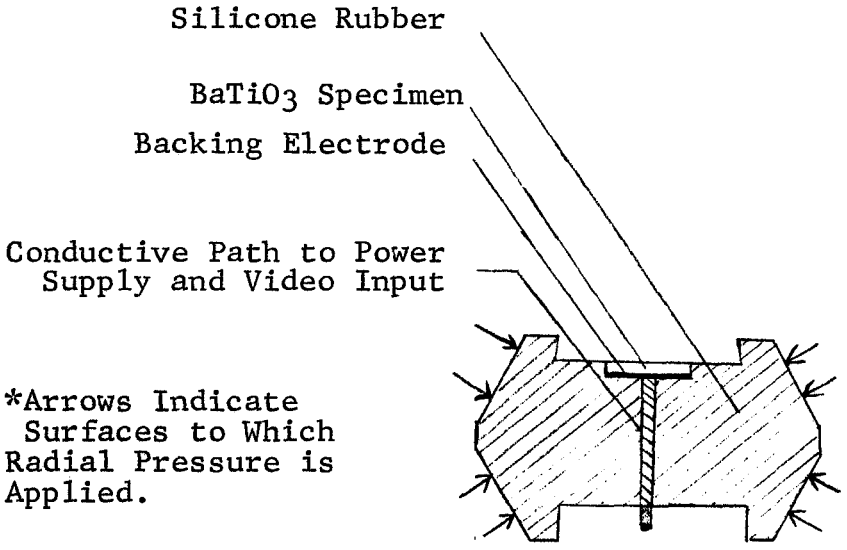

Fig. 21 $BaTiO_3$ SPECIMEN HOLDER

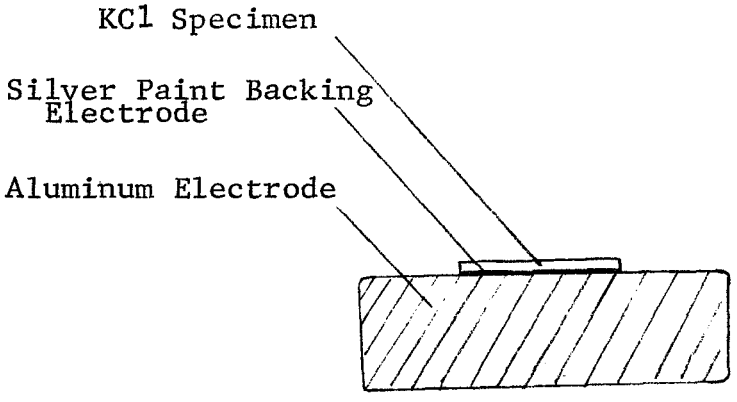

Fig. 22 KCl SPECIMEN HOLDER

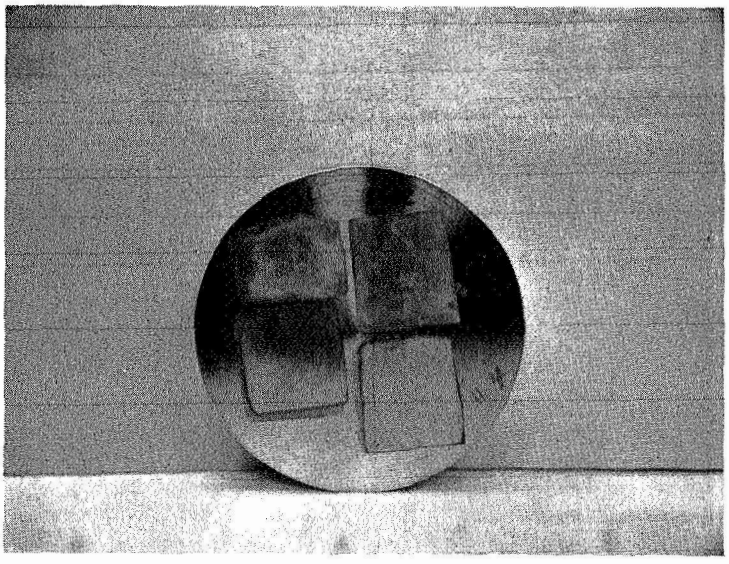

Fig. 23 SAMPLE HOLDER WITH FOUR KCl BICRYSTALS

specimen, then it may not be possible to separate these two effects and observe the dielectric properties. In order to achieve this objective the following was done:

a) The noise due to external pickup and internal generating sources was reduced to about 1.5×10^{-10} amperes. (This can be reduced further, but with difficulty.)

b) The specimens were ground as thin as possible to make the ratio of surface resistance to bulk resistance as large as possible, and to increase the capacitance per unit area to as large a number as possible which minimizes the secondary redistribution effects.

c) The "ground" reference grid was placed as close to the front surface of the specimen as possible, to minimize the effects that potential gradients on the surface of the sample would have on the charging of areas adjacent to these graded areas and further, to reduce secondary electron redistribution.

A conductivity profile was carried out on KCl bicrystal #1 (twist 10°). Figures 24 (a), (b), and (c) are photographs of the isometric display of the spatial conductivity of the specimen at different delay times (i.e., between two successive scans). In Figure 24 (a) the delay between frames was 5.05 sec. This delay time was found to be insufficient to permit enough leakage to occur to differentiate between the electrical conductivity of the grain and boundary regions. Figures 24 (b) and (c) are conductivity displays with delay times of about 1 min and 3 min, respectively. The results indicate that with a delay time of 1 min and greater, the grain-boundary conductivity can be differentiated from that of the grains.

Figures 25 and 26 are single line scans across the grain-boundary corresponding to scan delays of 2 and 3 min, respectively. The beam current was ostensibly the same in both photographs, so that the relative heights of the peaks across the grain-boundary region are most likely an indication of the surface

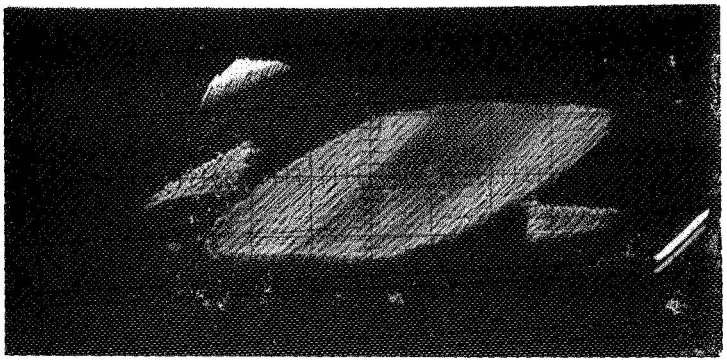

(a)

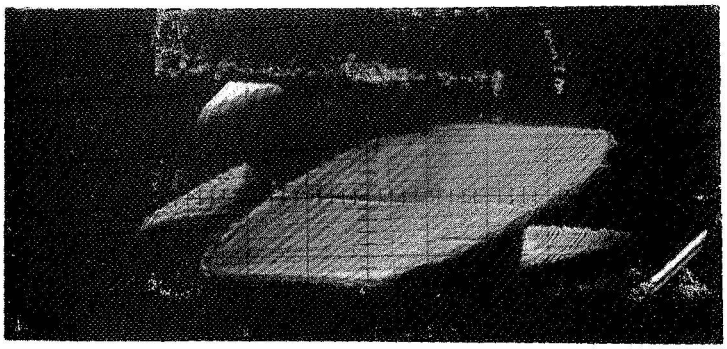

(b)

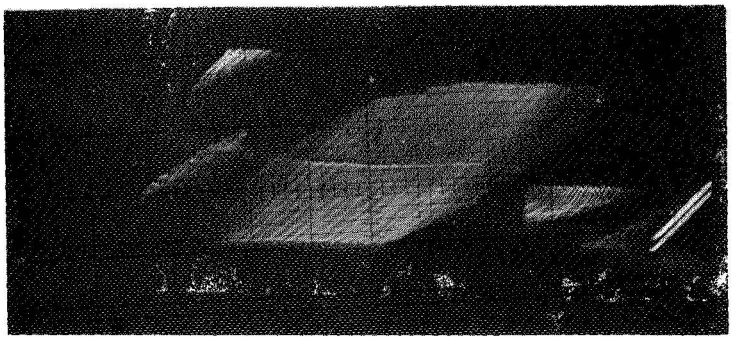

(c)

Fig. 24 - SPATIAL CONDUCTIVITY PROFILE OF KC1 BICRYSTAL SPECIMEN #1
(a) Scan repetition rate, 5.05 sec
(b) Scan repetition rate, 1.1 min
(c) Scan repetition rate, 3.1 min

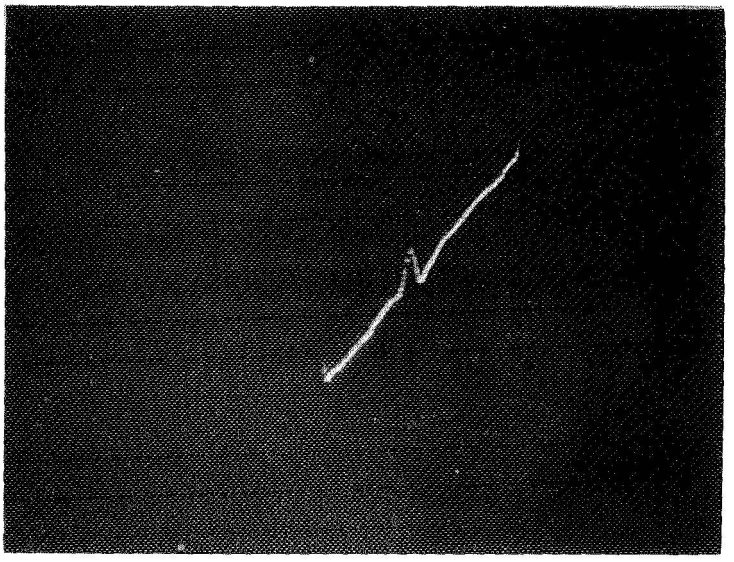

Fig. 25 - SINGLE LINE CONDUCTIVITY SCAN ACROSS THE GRAIN BOUNDARY OF KCl SPECIMEN #1 (Scan delay, 2 min)

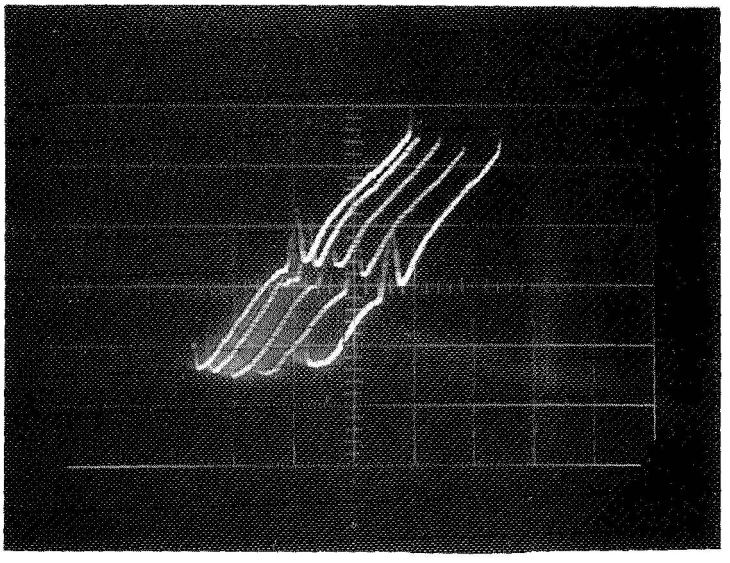

Fig. 26 - SINGLE LINE CONDUCTIVITY SCANS ACROSS THE GRAIN BOUNDARY OF KCl SPECIMEN #1 (Scan delay of trace at left, 3 min)

potentials of the specimen which are related to the local bulk conductivity -- assuming the local transverse surface resistivity is to be very high. From Figures 25 and 26 it is evident that an increase in delay time increases the intensity of the conductivity peak in the direction of the higher differential conductivity. This tends to confirm the fact that the conductivity profile peak at the grain-boundary is most probably a true conductivity effect, rather than being due to secondary emission effects.

The results further indicate that in KCl bicrystal specimen #1, the grain-boundary region has an electrical conductivity sufficiently different and higher than the grains.

An attempt was made to obtain a permittivity profile of $BaTiO_3$ specimen #1. This profile, in an intensity modulated isometric display, is shown in Figure 27. The results indicate that there are regions of differing dielectric constant, the darker regions indicating a higher dielectric constant. Figure 28 shows the arrangement and distribution of the grains in the test specimen. The areas of differing permittivity in Figure 27 closely match those regions representing individual grains in the specimen. This tends to indicate that different regions in the multicrystalline specimen have different permittivities depending upon the orientation of the grains.

Quantitative data on the conductivity or permittivity profile for the $BaTiO_3$ specimen has not yet been generated; however, modifications of the preamplifier input for dc response and the acquisition of an electron gun with a smaller beam spot size have been accomplished within this program. It is hoped that this will allow a more quantitative measurement to be made.

It must be stressed that these measurements of permittivity as a function of position are preliminary, qualitative measurements. Sizeable negative potentials existed on the front surface of the specimen. All regions on the specimen did not charge up to secondary emission equilibrium within one raster

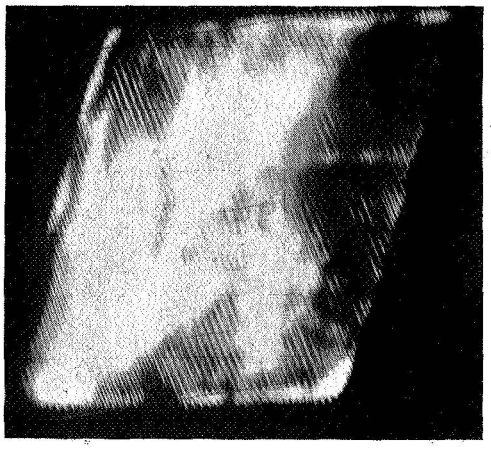

Fig. 27 INTENSITY MODULATED DISPLAY OF THE PERMITTIVITY PROFILE OF MULTICRYSTALLINE $BaTiO_3$ SPECIMEN (NO. 1)

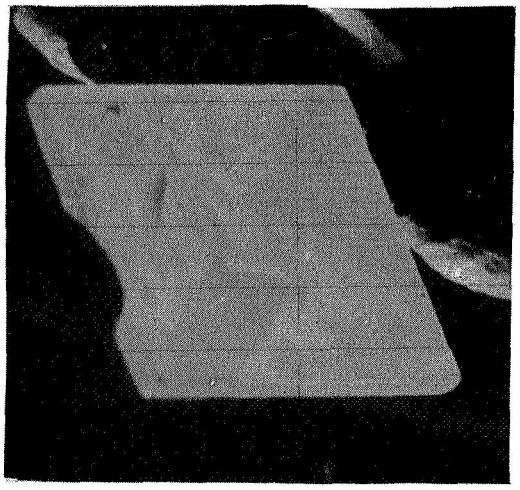

Fig. 28 OPTICAL PHOTOMICROGRAPH OF MULTICRYSTALLINE $BaTiO_3$ SPECIMEN (NO. 1)

scan (the darkest regions), as was shown by subsequent scans. The diameter of the electron beam was certainly quite large compared to the width of the grain-boundary.

However, these preliminary results are encouraging for they indicate that the EBS technique can be used to study dielectric characteristics of the grains and boundary regions in $BaTiO_3$.

2. Effects of Boundary Orientation and Environment on Dielectric Properties

Conductivity profiles of KCl bicrystal specimens with the following misorientations were evaluated, both under desiccated and nondesiccated conditions:

Bicrystal No.	Twist	Tilt
1	10°	0°
2	12°	0°
3	16°	0°
4	0°	30°

The results indicated the following:

1. The conductivity of the grain-boundary (gb) region is higher than that of the grain (g), and the ratio σ_{gb}/σ_g increases with increasing boundary twist misorientations in specimens exposed to "normal" atmospheric conditions (i.e., containing water vapor).

2. σ_{gb}/σ_g of the KCl twist bicrystals appears to approach unity as the storage time of the specimens under desiccating conditions (vacuum $\sim 10^{-5}$ torr) is extended over several hundred hours (>500 hrs). An EBS conductivity profile under these conditions produces no discernable change in conductivity as a function of position across the specimen, even in the region of the gb. The change in conductivities with time is shown in Figure 29.

This is a real observation provided the surface conductivity is of the same order as, or smaller than σ_{gb}. The contribution to the time constant due to the surface conductivity is,

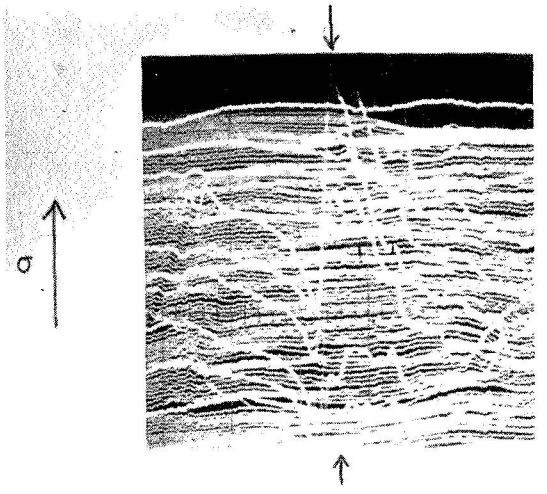

(a) Stored in Vacuum for ~ 3 hr.
Scan Delay Time 2 min.

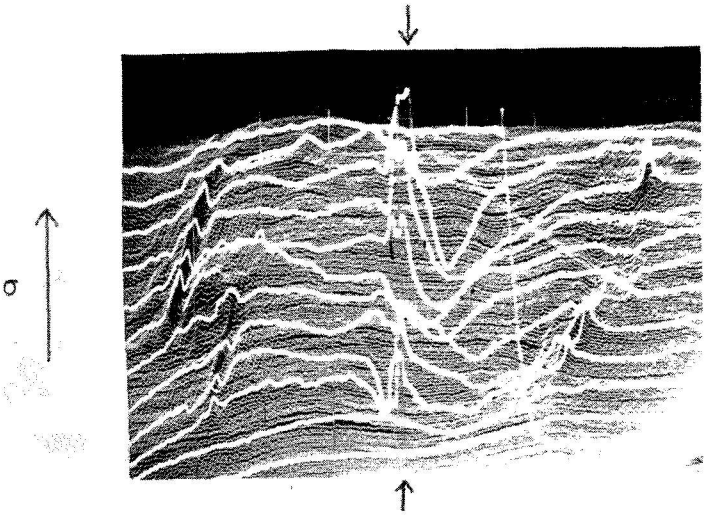

(b) Stored in Vacuum for ~ 30 hr.
Scan Delay Time 3 min.

Fig. 29 CONDUCTIVITY PROFILE ACROSS A GRAIN-BOUNDARY IN KCl BICRYSTAL (Twist 12°)
(Arrows Indicate Position of Grain-Boundary)

in any event, of the same order or smaller than those contributions due to bulk conductivities, with vacuum storage times such that $\sigma_{gb}/\sigma_{g} > 1$.

3. A grain-boundary of high tilt ($\sim$30°) misorientation did not show any noticeable difference in conductivities of the gb region and the adjoining grains, as shown in Figure 30.

4. Exposure of twist boundaries to atmospheric conditions, in particular water vapor, increases the effective width of the boundary region whose conductivity is higher than that of the grains. This increase in effective width may be due to the increased surface conductivity in the hydrated state which sets up surface voltage gradients, or it may be due to the interaction of adsorbed hydroxyl groups at the grain-boundary with ionic defects in the KCl crystal.

5. Preliminary data on permittivity (ϵ) profiles indicates that for both tilt and twist boundaries the ratio $\epsilon_{gb}/\epsilon_{g}$ increases as a function of exposure to atmospheric (hydrating) conditions. For specimens stored under good desiccating conditions (100 hrs at 10^{-5} torr), $\epsilon_{gb}/\epsilon_{g} \approx 1$.

The results obtained indicate that water vapor can cause significant differences in the electrical properties of ionic materials by interacting with grain-boundaries. It also seems that screw dislocations (characteristic of twist boundaries), may be significant in enhancing the differences in conductivities between grain-boundaries and grains in ceramic materials, such as potassium chloride.

D. Conclusions

The electron beam scanning results indicate that grain-boundaries in ionic materials such as KCl, have conductivities differing from those of the grain depending upon their misorientation. For twist boundaries, the grain-boundary conductivity is higher than that of the grains and this difference increases

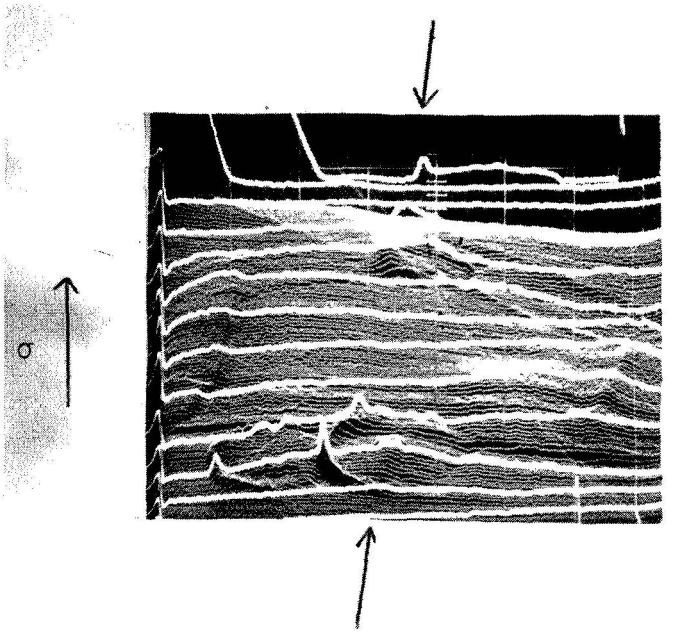

Fig. 30 CONDUCTIVITY PROFILE ACROSS A GRAIN-BOUNDARY IN KCl BICRYSTAL (Tilt 30°)
(Arrows Indicate Position of Grain-Boundary)
Scan Delay Time 8 min.

with increasing twist. No such difference in the grain-boundary and grain conductivities were found for a high angle tilt boundary. The observed increase in twist grain boundary conductivities is, to a significant extent, due to the interaction of hydroxyl groups with defects in the boundary region.

The EBS results also indicate that in $BaTiO_3$ ceramics the permittivity values in the grain-boundary region are significantly different from those in the grains.

While the observations made so far constitute only a beginning, they clearly indicate the utility of such EBS measurements in studying electronic and electrical characteristics of grain-boundaries and other interfaces, especially in microelectronics.

V. PERSONNEL

The principal investigator on this program was A. J. Mountvala. Strong contributory effort on the electron beam scanning work was provided by H. R. Marks. Additional assistance on sample preparation and dielectric loss tests was provided by W. R. Logan. Dr. S. L. Blum, Director of Ceramics Research, provided administrative supervision. The work reported herein was performed under the technical direction of Flight Instrumentation Division, Microelectronics Section, Langley Research Center.

Respectfully submitted,
IIT RESEARCH INSTITUTE

A. J. Mountvala
Senior Scientist
Ceramics Research

APPROVED:

M. A. Schwartz
Assistant Director
Ceramics Research

REFERENCES

1. Mountvala, A. J., "Characterization of Ceramic Materials for Microelectronic Applications", NASA Contract No. NAS1-6919, Summary Report (March 1968).

2. Anderson, P. J., Horlock, R. F., Oliver, J. F., "Interaction of Water with Magnesium Oxide", Trans Faraday Soc., 61(516) 2754-62 (1965).

3. Stuart, W. I., Whateley, T. L., "Adsorption of Water and Carbon Dioxide on Beryllium Oxide", Trans. Faraday Soc. 61(516) 2763-71 (1965).

4. Peri, J. B., "Infrared and Gravimetric Study of the Surface Hydration of Gamma-Alumina", J. Phys. Chem., 69 (1) 211-19.

5. Weyl, W. A., Terhune, N., Ceram. Age (August 1953).

6. Mountvala, A. J., "Characterization of Ceramic Particles", ONR Contract No. N00014-68-C-0305, First Semi-Annual Report (October 1968).

7. Mazdiyasni, K. S., Private communications.

8. Goswami, A. K., "Dielectric Properties of Unsintered Barium Titanate", J. Appl. Phys. 40(2) 619-24 (1969).

9. Seiwatz, H., "A Nondestructive Electron Beam Scanning System for Measuring Dielectric Properties Including Breakdown", Proceedings of the Fifty-First Meeting of the Juniper Committee, Sandia Corporation (May 1966).

NASA CR-66817

DISTRIBUTION LIST

NAS1 8025

	Copies
NASA Langley Research Center Langley Station Hampton, Virginia 23365	
Attention: Research Program Records Unit, Mail Stop 122	1
Charles Husson, Mail Stop 470	25
Raymond L. Zavasky, Mail Stop 117	1
NASA Ames Research Center Moffett Field, California 94035	
Attention: Library, Code 202-3	1
Thomas Fryer, Mail Stop 213-4	1
NASA Flight Research Center P. O. Box 273 Edwards, California 93523	
Attention: Library	1
D. Veatch, Division D	1
NASA Goddard Space Flight Center Greenbelt, Maryland 20771	
Attention: Library	1
A. Franta, Code 722	1
D. Schaeffer, Code 711	1
Jet Propulsion Laboratory 4800 Oak Grove Drive Pasadena, California 91103	
Attention: Library, Mail 111-113	1
D. Bergens	1
NASA Manned Spacecraft Center 2101 Webster Seabrook Road Houston, Texas 77058	
Attention: Library, Code BM6	1
S. Guadiand Code EE2	1
NASA Marshall Space Flight Center Huntsville, Alabama 35812	
Attention: Library	1
Dr. Aluis Holloday	1

NASA CR-66817

DISTRIBUTION LIST

NAS1 8025

	Copies
P. R. Mallory and Co., Inc. 3029 E. Washington Street Indianapolis, Indiana 46202 Attention: Mrs. Marjorie M. Ford, Librarian	1
NASA Wallops Station Wallops Island, Virginia 23337 Attention: Library	1
NASA Electronics Research Center 575 Technology Square Cambridge, Massachusetts 02139 Attention: Library W. C. Dunlap, Code C	1 2
NASA Lewis Research Center 21000 Brookpark Road Cleveland, Ohio 44135 Attention: Library, Mail Stop 60-3 John Sturman, Mail Stop 77-1	1 1
NASA John F. Kennedy Space Center Kennedy Space Center, Florida 32899 Attention: Code IS-CAS-42B	1
NASA Michoud Assembly Facility P. O. Box 26078 New Orleans, Louisiana 70126 Attention: Mr. Henry Quintin, Code I-Mich-D	1
National Aeronautics and Space Administration Washington, D. C. 20546 Attention: Library, Code USS-10 Dr. Robert Nash, Code RRS	1 3
NASA Scientific and Technical Information Facility P. O. Box 33 College Park, Maryland 20740	7 plus repro. reproducible